Reply to Referee #1

Dear Dr. Kokhanovsky,
We would like to thank you for the review and your constructive comments which helped to improve our manuscript.
Our point-by-point responses to the specific comments (in red) are given in blue and the modification made in the manuscript is presented in green. This document also includes a marked-up version of manuscript.

Best Regards,
Soheila Jafariserajehlou

#1 Comment to the Author:

The selection of the appropriate snow grain shape and size must be performed using both angular and spectral measurements. The authors discuss mainly the angular patterns. It is interesting to see how differ spectral reflectances for different best models shown in Table 2 and how they agree with spectral reflectance measurements at 14 Cloud Absorption Radiometer (CAR) spectral channels.

Author's response:

This is definitely true; it would be very interesting to see the change of reflectance in the wide spectral range of CAR. Unfortunately, the investigation of all wavelengths was not considered in the scope of our study mainly because of two problems:

1. The variation of ice absorption with the increase of wavelength in the near IR range: This means that the photon penetration depth in snow layer will depend on the wavelength. Considering our assumption in SCIATRAN: a vertically homogeneous snow layer, we will obtain for different wavelengths different effective radius of ice crystals. With these results, we could only confirm that a snow layer is vertically in-homogeneous. However, we know this without additional calculations. Therefore, we would consider the reflectance at

wavelengths in more near IR range only if we could assume vertically inhomogeneous snow layer and formulate the inverse problem with respect to the vertical profile of ice crystal effective radius. However, the consideration of this problem and solution of its inverse problem is out of scope of this manuscript but we will definitely consider it in the future studies.

2. Not all of the 14 spectral channels of CAR were active during all of our measurements.

Modifications: -

#2 Comment to the Author:

Please, list the CAR channels in the paper.

Author's response:

Thanks for reminding this point to us. We added a table including all channels of CAR and their bandwidth.

Modification: Table 2. Summary of CAR wavelengths and bandwidth.

Channel number	Central wavelengths in μm	Bandwidth in nm
1	0.480	21
2	0.687	26
3	0.340	9
4	0.381	6
5	0.870	10
6	1.028	4
7	0.609	9
8	1.275	24
9	1.554	33
10	1.644	46
11	1.713	46
12	2.116	43
13	2.203	43
14	2.324	48

#3 Comment to the Author:

Asymmetry parameters in the visible must be given for all cases shown in Table 2.

Author's response: Done. We added asymmetry parameter to table 2 (now is 3).

Modification: table 3.

Ice crystal habit	Asymmetry parameter		Retrieved effective radius (μm)		Old snow		Fresh snow	
	Old snow	Fresh snow	Old snow	Fresh snow	Bias (%)	RMSE (%)	Bias (%)	RMSE (%)
Fractal	0.825	0.827	69.37	76.06	3.50	9.75	13.16	14.69
Droxtal	0.856	0.863	94.48	106.95	0.87	25.54	10.10	34.14
Column	0.873	0.877	74.71	80.49	2.17	7.32	12.36	15.72
Hollow column	0.884	0.888	67.32	72.85	2.80	11.15	13.66	15.14
Aggregate of 8 columns	0.844	0.849	98.83	107.62	2.79	6.97	11.85	18.27
Plate	0.923	0.942	38.93	61.44	-0.44	21.47	11.68	16.99
Aggregate of 5 plates	0.874	0.877	78.02	83.41	1.82	10.34	11.23	12.85
Aggregate of 10 plates	0.893	0.893	65.36	69.28	2.34	13.91	11.52	13.16
Hollow-bullet rosette	0.887	0.889	67.01	73.28	2.16	9.99	12.71	15.16

#4 Comment to the Author:

The authors assume clean snow. I think, the authors must show some evidence in the paper that the measured spectra have not been affected by possible snow pollution.

Author's response:

Unfortunately, there was no measurement of the snow impurities such as black carbon collocated to the CAR measurements. Nevertheless, to understand the conditions at

Barrow better and having a picture of existing aerosol there, we tried to collect information by looking at:

1) Long term continuous measurements of chemical and optical properties of aerosol at Barrow, Alaska (Kokhanovsky and Tomasi, 2020: chapter 4: Udisti et al., 2020): Based on 3 years continuous measurements, during the haze season (January to April), sea salt plays the dominant role in controlling light scattering in wintertime, and non-sea salt sulfate in spring. As can be seen from the Fig. A below, the average contribution of black carbon is very small compared to other aerosol types at Barrow.

2) Aeronet station at Barrow: Although from Aeronet we could not have information about the chemical composition of aerosol, the AOD values before old snow case (7th of April) does not show a significant episodic aerosol event by which snow could be polluted significantly. Our second case study (15th of April) is over fresh fallen snow in which the possibility of being affected by pollutants is even less.

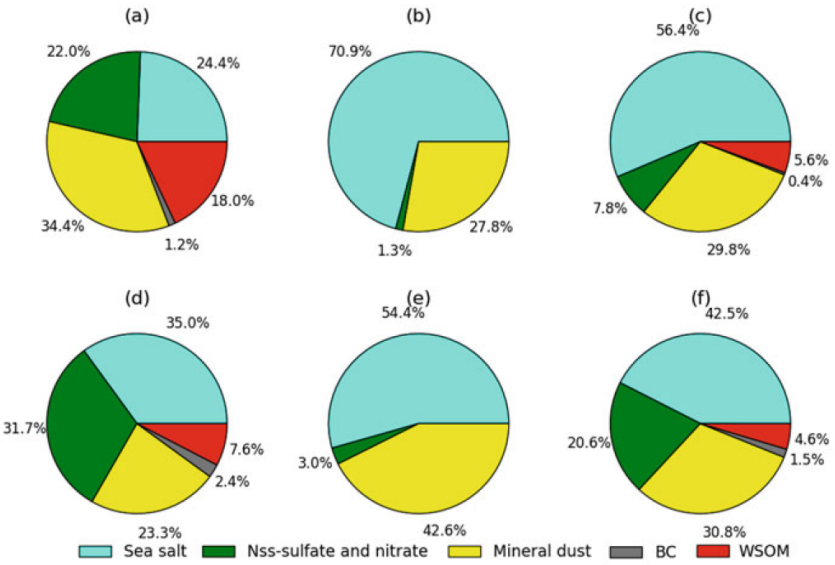

Fig. A: Average composition diagrams of the ground-level particulate matter sampled at Barrow during different seasonal periods. Summer time (June-September): (a), (b), (c): sub-micrometric, super micrometric and overall aerosol particles sampled;

In winter time (October-May):(d), (e), (f): sub-micrometric, super-micrometric and overall aerosol particles sampled respectively. Different colours are used to indicate the main particulate matter constituents (sea salt, nss-sulfate and nitrate, mineral dust, black carbon (BC), and water-soluble organic matter (WSOM).

Modifications: line 225-233.

Aerosol condition and its chemical and optical properties have been measured continuously at Barrow, Alaska, during different seasonal periods (Quinn et al., 2002). Previous studies indicate the largest contribution from sea salt, non-sea-salt sulfate and mineral dust. The average contribution of black carbon is very small compared to other aerosol types (Udisti et al., 2020). The increase on nss-sulfate in January to May is the long-range transport of anthropogenic primary nss sulfate besides the long-range transport of anthropogenic SO2 and its photo-oxidization to nss-sulfate with increase of light levels, and the local production of biogenic nss-sulfate.

Udisti, R., Traversi, R., Becagli, S., Tomasi, C., Mazzola, M., Lupi, A., and Quinn, P. K.: Arctic Aerosols in: Physics and Chemistry of the Arctic Atmosphere, edited by: Kokhanovsky, A. A., Tomasi, C., Springer Nature Switzerland AG, Cham, Switzerland, 2020.

Quinn, P. K., Miller, T. L., Bates, T. S., Ogren, J. A., Andrews, E., & Shaw, G. E.: A 3-year record of simultaneously measured aerosol chemical and optical properties at Barrow, Alaska., J. Geophys. Res., Atmos., 107(D11), AAC 8-1–AAC 8-15, 2002

#5 Comment to the Author:

Line 4, leads–>lead;

Author's response: Done.

Modification: (moved to line 58): However, the current differences between simulated and measured reflectance in a coupled snow-atmosphere system, lead to ….

#6 Comment to the Author:

line 32, to be –>is;

Author's response: Done.

Modifications: line 30…we find that for a surface covered by old snow, the Pearson correlation coefficient, R, between measurements and simulations is 0.98 (R2 ~ 0.96).

#7 Comment to the Author:

line 46 (AA);

Author's response: Done.

Modifications: line 51. This phenomenon is known as the Arctic Amplification (AA) (Serreze and Barry, 2011).

#8 Comment to the Author:

line 204, is reference available?

Author's response:

Yes, when we wrote this manuscript the reference was under preparation but now it is published:

https://www.sciencedirect.com/science/article/abs/pii/S0022407320302442

Modifications: line 260 and reference updated at line 685:

Pohl, C., Rozanov, V. V., Mei, L., Burrows, J. P., Heygster, G., Spreen, G.,: Implementation of an extensive ice crystal single-scattering property database in the radiative transfer model SCIATRAN, J. Quant. Spectrosc. Ra., 253, https://doi.org/10.1016/j.jqsrt.2020.107118, 2020.

#9 Comment to the Author:

Line 210, did you assume rough Koch crystals?

Author's response: Yes. We assumed rough Koch crystals.

Modifications: -

#10 Comment to the Author:

line 240, the wavelength of 1.24 microns is more suitable for the grain size retrieval (larger sensitivity to the grain size);

Author's response:

In the retrieval algorithm, we assume a vertically homogeneous snow layer. To decrease the photon penetration depth and estimate the effective radius of ice crystals near the top of snow layer the wavelength 1.65 micron with stronger absorption was selected. The measurement errors in this spectral channel cannot significantly decrease the accuracy of inverse problem solution. Figure 6 of the manuscript clearly demonstrates dependence of RMSE on the selected shape and even on roughness of ice crystal. This confirms that the sensitivity of reflectance with respect to the effective radius is high enough.

Modifications: -

#11 Comment to the Author:

line 250, matrix->function

Author's response: Done.

Modifications: line 310:

The BRF properties of snow at 1.649 μm are closer to that for single scattering behavior and it is linked to the phase function, which strongly depends on the shape of ice crystals.

#12 Comment to the Author:

line 271, a priori

Author's response: Done.

Modifications: line 337:

The large range of changes of the reflectance when using different ice crystal sizes in both the principal and cross planes highlights the importance of having accurate a priori

knowledge or estimation of size of the ice crystals and their shapes to simulate accurately measurements.

#13 Comment to the Author:

line 276, remove 'on the snow layer'

Author's response: Done.

Modifications: line 345: The incident radiation is composed of direct sunlight and the diffuse radiation from the sky.

#14 Comment to the Author:

line 295, remove #please#.

Author's response: Done.

Modifications: line 365: For more information on aerosol typing used in this study, see Levy et al. (2007).

Reply to Referee #2

We would like to thank you for the review and your constructive comments which helped to improve our manuscript.
Our point-by-point responses to the specific comments (in red) are given in blue and the modification made in the manuscript is presented in green. This document also includes a marked-up version of manuscript.

Best Regards,
Soheila Jafariserajehlou

General comments

#1 Comment to the Author

After reading the manuscript, its scope is still not entirely clear to me: (1) Is it about the description of a novel algorithm for the simultaneous retrieval of the snow grain size and ice crystal shape? In that case, it is a bit confusing to me that you moved the entire description of this algorithm to the appendix, while at the same time, the sentence 'we present a novel two-stage snow grain morphology [...] retrieval algorithm' is part of the abstract. If you want to focus more on the description of this algorithm, maybe it is worth to think about moving it to a more prominent spot within the manuscript. (2) Is it about the sensitivity of the radiative transfer model to the snow and atmospheric input parameters? (3) Or is the main focus the comparison of BRF simulations with the CAR measurements?
To be clear, I do think that all three parts are important contributions. However, it is important that each part presented in the manuscript is investigated thoroughly. And until now, each part is missing some pieces in my point of view and I will give more details on that further below in the specific comments. However, this lack of focus seems to already appear in the title, which reads very confusing and imprecise to me. The

authors of course wanted to include all pieces, but this came at the cost of the readability and conciseness.

Author's response:

We agree with your comment, we need to highlight more the main focus of our paper. As you said all three parts are very important, we tried to bring necessary information and avoid of representing too much details. But we do understand your point and therefore, we modified the abstract and the title of our paper.

We would like to emphasize that the goal of our study was to achieve the best possible simulated reflectance in a snow-atmosphere system using our radiative transfer model. Testing the sensitivity of reflectance to snow and atmospheric parameters was a step to show the importance of snow morphology and atmosphere.

To achieve our goal and minimize the difference between simulation and observation, we tried to have the best possible estimation about surface and atmosphere. Therefore, the use of snow grain size/shape retrieval algorithm was our second priority and for this reason we put the algorithm itself in the appendix to keep the structure of manuscript in the frame of main goal.

We agree that the sentence "we present a novel two stage algorithm in the abstract", and the title of our paper may be confusing. To solve this problem we applied the following changes.

Modifications:

Title: Simulated reflectance above snow, constrained by airborne measurements of solar radiation: Implications for the snow grain morphology in the Arctic.

Line 8-11:

In this paper, we simulate the reflectance in a snow-atmosphere system using the phenomenological radiative transfer model SCIATRAN and compare the results with that of airborne measurements. To minimize the differences between measurements and simulation, we determine and employ the key atmospheric and surface parameters such as snow morphologies (or habits)…

#2 Comment to the Author

Another important part is the terminology used throughout the manuscript. As you are referencing Schaepman-Strub et al. (2006) extensively in Sect. 2 'Theoretical background', I recommend you also stay consistent in the use of reflectance terminology. Equation 4 defines a reflectance factor according to Schaepman-Strub et al. (2006) and should be named 'reflectance factor' and not 'reflectance' as stated for example on Page5 Line143. Otherwise, this quickly becomes very confusing to the reader as it is very important to stay precise to differentiate between the different reflectance quantities. I mention some occasions where 'reflectance' should be replaced with 'reflectance factor' below in the Technical corrections. However, the authors should double check and change it in the entire manuscript.

Author's response:

Thanks for pointing this out. Yes, we should stay consistent with respect to terminology. We changed reflectance to "reflectance factor" in every place (text and figures) where we refer to calculated/simulated reflectance factor using Eq. 4.

Modifications:

Please see the manuscript.

#3 Comment to the Author

Unfortunately, some parts of the manuscript are quite difficult to read and the use of English should be improved to make the line of argumentation easier to follow. I gave some recommendations in the comments, but I think the authors should check the entire manuscript to foster reading comprehension.

Author's response:

We applied all of your comments and we also tried to improve the readability of our manuscript.

Modifications:

Please see the technical comments with details and manuscript.

#4 Comment to the Author

One of the most pressing aspects is the lack of accounting for measurement uncertainties. A detailed discussion of the measurement and retrieval uncertainties for the BRF measurements with the CAR is missing. Also, every time CAR measurements are shown, uncertainty bars need to be included (especially Figures 5 and 6, see also specific comments below). This also applies to the a priori estimation of the effective radius of the snow grains (Figure 7), and the scatter plots in Figure 10. I understand that adding uncertainty bars for the simulations in Figure 3 is not applicable as the plot is already very busy. However, as you even test the sensitivity of the simulations with respect to, e.g. how absorbing the aerosols are, at least some uncertainty estimates should be given within the text. The uncertainty discussion is especially important as it might influence conclusions drawn from the RMSE analysis: if all influencing factors are named and properly quantified, non-significant differences in the RMSE of 0.4 % (Figure 5) between two different ice crystal shapes should not be relevant and influence a decision for a specific ice crystal shape being used in the simulations.

Author's response:

We agree that uncertainty of measurements, simulation and retrieval are very important and should be plotted and discussed in our manuscript. Thanks for pointing this out.

The uncertainty of CAR measurements is within 5% based on a comprehensive study done in NASA in 2007 (Dr. Gatebe from NASA / co-author of this paper). We added uncertainty envelopes to measurements in Fig. 5, 6 (now they are 6 and 7) and also in the text.

The uncertainty of effective radius retrieval is estimated to be ~10% on the base of optimal estimation technique. We also added uncertainty envelope to the plot in Fig.7 (now is 8) and text accordingly.

The uncertainty of our radiative transfer calculations is estimated to be in the range of 0.1 % and we did not add it to our plots because of being too small, because it can't be seen. However, we added this uncertainty to the text of manuscript.

Modifications:

Line 385 – 387:

Fig. 6 shows one example of the comparison between measured and simulated reflectance factor at principal and cross planes. The absolute uncertainty of CAR measurements is within 5% and shown by uncertainty envelope. The accuracy of our radiative transfer calculations is estimated to be in the range of 0.1 %.

Line 432-434:

The uncertainty of effective radius retrieval is estimated to be ~10% on the base of optimal estimation technique and shown by gray envelope in Fig. 8.

Figure 6:

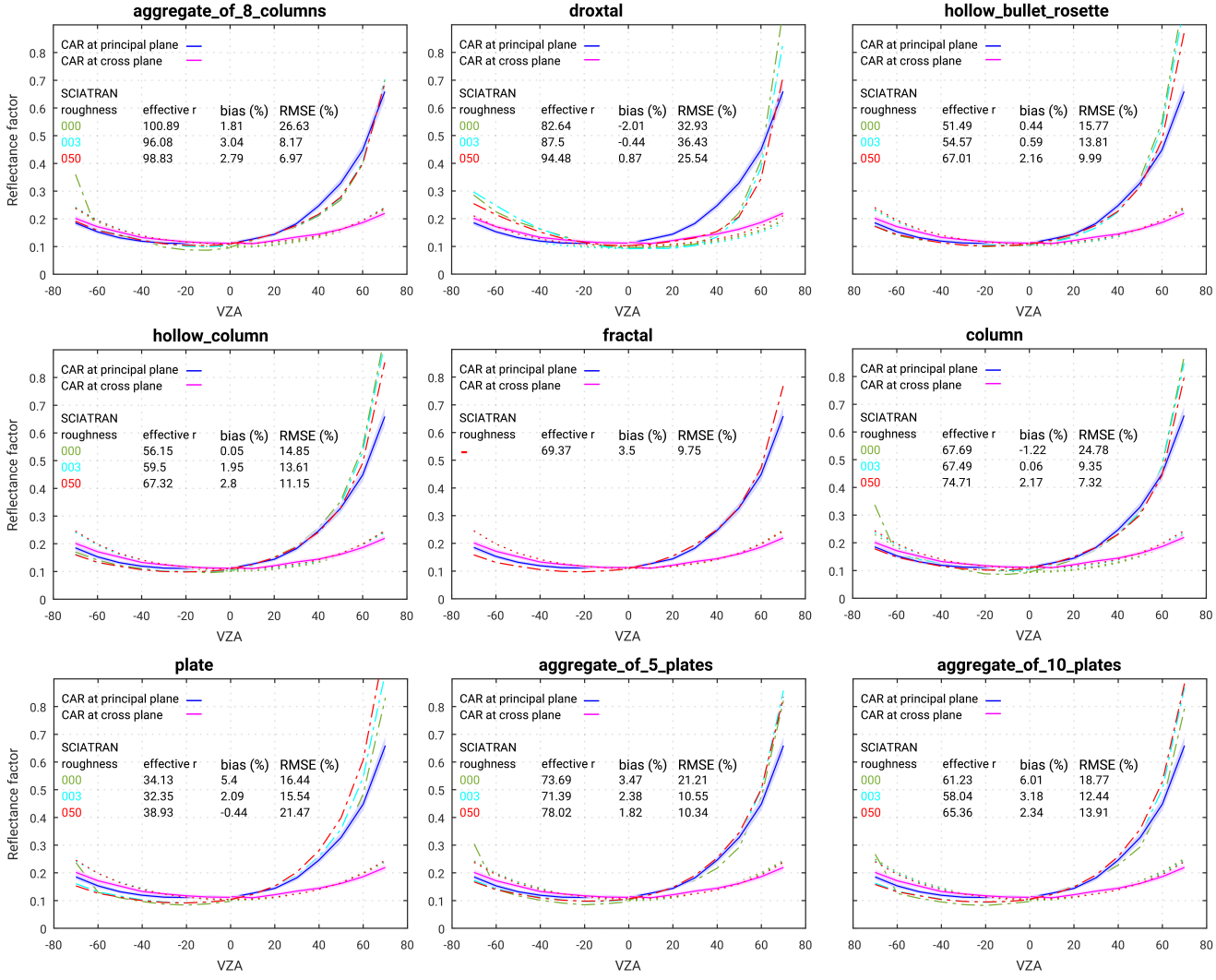
aggregate_of_8_columns
CAR at principal plane
CAR at cross plane
SCIATRAN
roughness effective r bias (%) RMSE (%)
000 100.89 1.81 26.63
003 96.08 3.04 8.17
050 98.83 2.79 6.97
droxtal
CAR at principal plane
CAR at cross plane
SCIATRAN
roughness effective r bias (%) RMSE (%)
000 82.64 -2.01 32.93
003 87.5 -0.44 36.43
050 94.48 0.87 25.54
hollow_bullet_rosette
CAR at principal plane
CAR at cross plane
SCIATRAN
roughness effective r bias (%) RMSE (%)
000 51.49 0.44 15.77
003 54.57 0.59 13.81
050 67.01 2.16 9.99
hollow_column
CAR at principal plane
CAR at cross plane
SCIATRAN
roughness effective r bias (%) RMSE (%)
000 56.15 0.05 14.85
003 59.5 1.95 13.61
050 67.32 2.8 11.15
fractal
CAR at principal plane
CAR at cross plane
SCIATRAN
roughness effective r bias (%) RMSE (%)
- 69.37 3.5 9.75
column
CAR at principal plane
CAR at cross plane
SCIATRAN
roughness effective r bias (%) RMSE (%)
000 67.69 -1.22 24.78
003 67.49 0.06 9.35
050 74.71 2.17 7.32
plate
CAR at principal plane
CAR at cross plane
SCIATRAN
roughness effective r bias (%) RMSE (%)
000 34.13 5.4 16.44
003 32.35 2.09 15.54
050 38.93 -0.44 21.47
aggregate_of_5_plates
CAR at principal plane
CAR at cross plane
SCIATRAN
roughness effective r bias (%) RMSE (%)
000 73.69 3.47 21.21
003 71.39 2.38 10.55
050 78.02 1.82 10.34
aggregate_of_10_plates
CAR at principal plane
CAR at cross plane
SCIATRAN
roughness effective r bias (%) RMSE (%)
000 61.23 6.01 18.77
003 58.04 3.18 12.44
050 65.36 2.34 13.91
Reflectance factor
VZA

Figure 7:

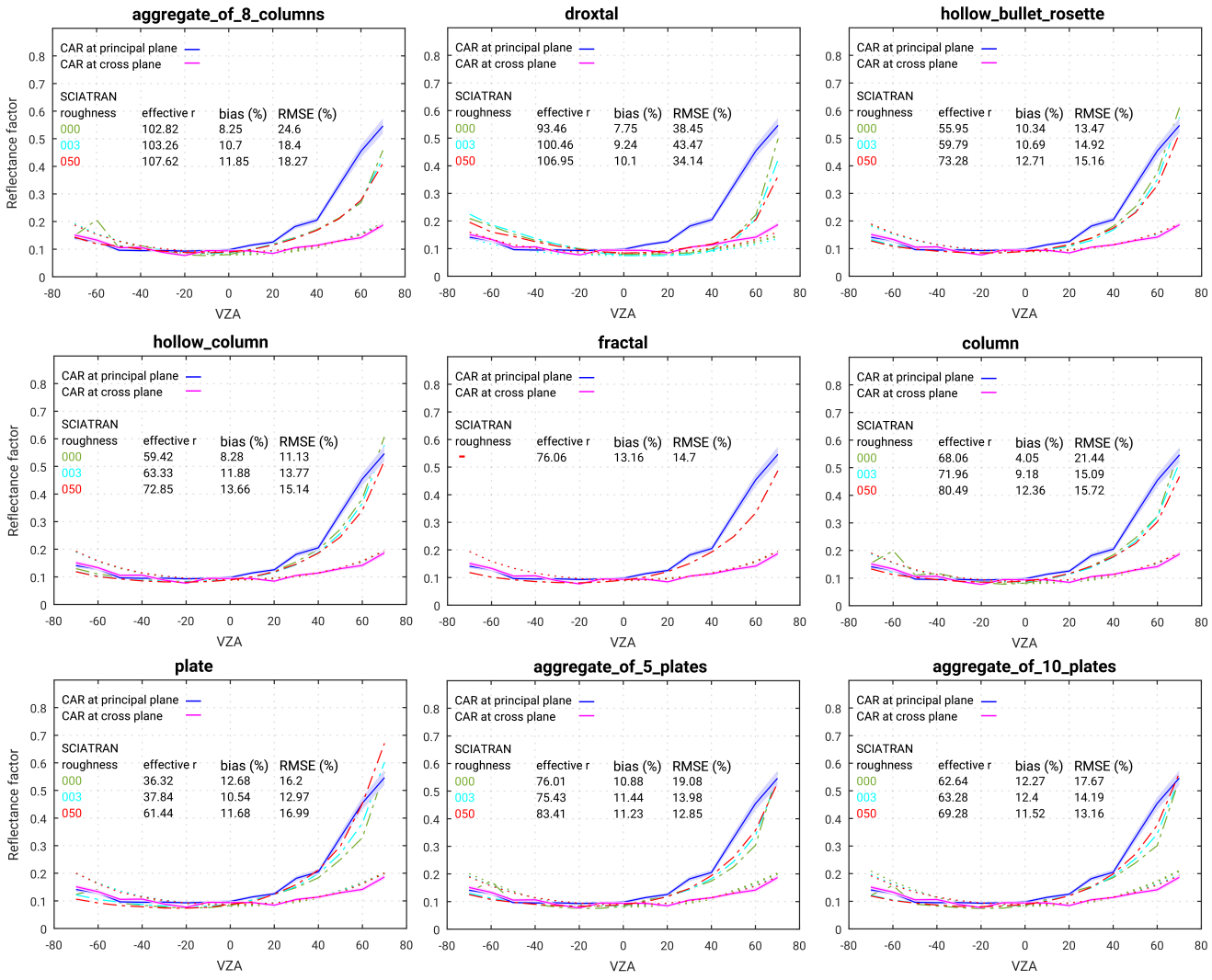
aggregate_of_8_columns
CAR at principal plane
CAR at cross plane
SCIATRAN
roughness effective r bias (%) RMSE (%)
000 102.82 8.25 24.6
003 103.26 10.7 18.4
050 107.62 11.85 18.27
droxtal
CAR at principal plane
CAR at cross plane
SCIATRAN
roughness effective r bias (%) RMSE (%)
000 93.46 7.75 38.45
003 100.46 9.24 43.47
050 106.95 10.1 34.14
hollow_bullet_rosette
CAR at principal plane
CAR at cross plane
SCIATRAN
roughness effective r bias (%) RMSE (%)
000 55.95 10.34 13.47
003 59.79 10.69 14.92
050 73.28 12.71 15.16
hollow_column
CAR at principal plane
CAR at cross plane
SCIATRAN
roughness effective r bias (%) RMSE (%)
000 59.42 8.28 11.13
003 63.33 11.88 13.77
050 72.85 13.66 15.14
fractal
CAR at principal plane
CAR at cross plane
SCIATRAN
roughness effective r bias (%) RMSE (%)
- 76.06 13.16 14.7
column
CAR at principal plane
CAR at cross plane
SCIATRAN
roughness effective r bias (%) RMSE (%)
000 68.06 4.05 21.44
003 71.96 9.18 15.09
050 80.49 12.36 15.72
plate
CAR at principal plane
CAR at cross plane
SCIATRAN
roughness effective r bias (%) RMSE (%)
000 36.32 12.68 16.2
003 37.84 10.54 12.97
050 61.44 11.68 16.99
aggregate_of_5_plates
CAR at principal plane
CAR at cross plane
SCIATRAN
roughness effective r bias (%) RMSE (%)
000 76.01 10.88 19.08
003 75.43 11.44 13.98
050 83.41 11.23 12.85
aggregate_of_10_plates
CAR at principal plane
CAR at cross plane
SCIATRAN
roughness effective r bias (%) RMSE (%)
000 62.64 12.27 17.67
003 63.28 12.4 14.19
050 69.28 11.52 13.16
Reflectance factor
VZA

Figure 8:

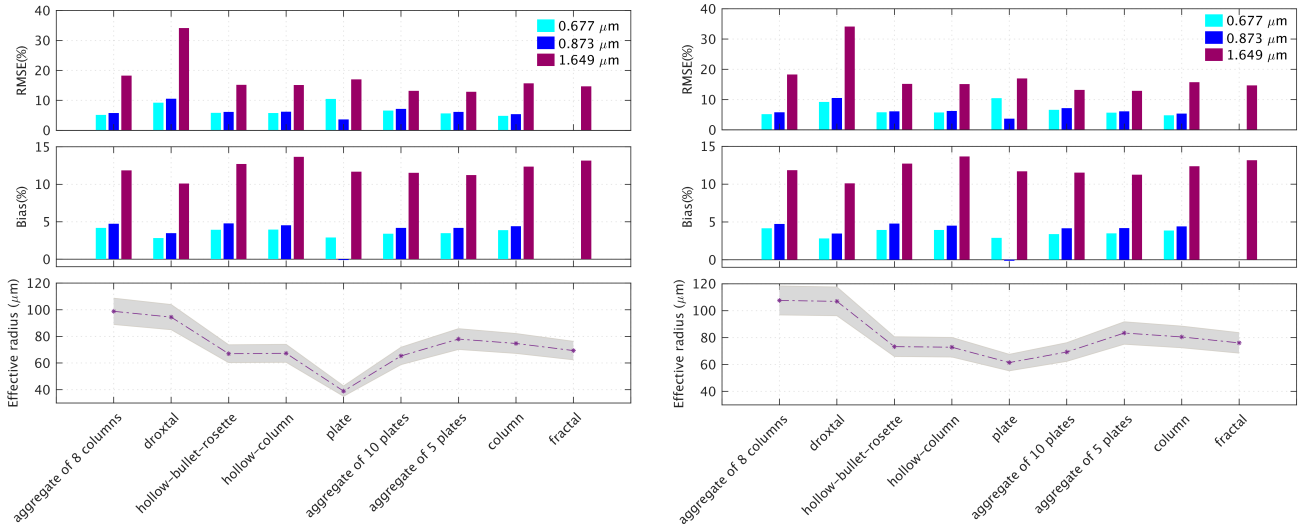

#5 Comment to the Author

The snow grain size is given in terms of the maximum extent within the manuscript. Although the physical size of a snow grain is traditionally defined by the length of the largest extension of the crystal, in terms of radiative properties the optical-equivalent snow grain size is way more important. It is defined as the radius of a collection of spheres with the same total volume and surface area compared to the actual nonspherical snow grain (see e.g. Grenfell and Warren, 1999; Neshyba et al., 2003). Displaying the reflectance factor for different crystal shapes and sizes in Figure 3, one could assume that the same crystal sizes are comparable between the different shapes. However, from a radiative point of view, this is not true, as each size (largest extent in

your case) is defined differently. I recommend using an optical-equivalent snow grain size in Figure 3 instead of the largest extension.

Author's response:

Yes, for this figure and relevant explanation we used the maximum length (but not for the retrieval of snow grain size). We agree that the maximum length is not giving the full picture. We thought maximum length would give a better/easier imagination of grain sizes to the readers when comparing different shape. But we understand your point and so added the effective radius besides maximum length to this figure (Fig. 4). We explained this new column in the caption and gave its definition within the manuscript.

Modifications:

We updated Fig. 4.

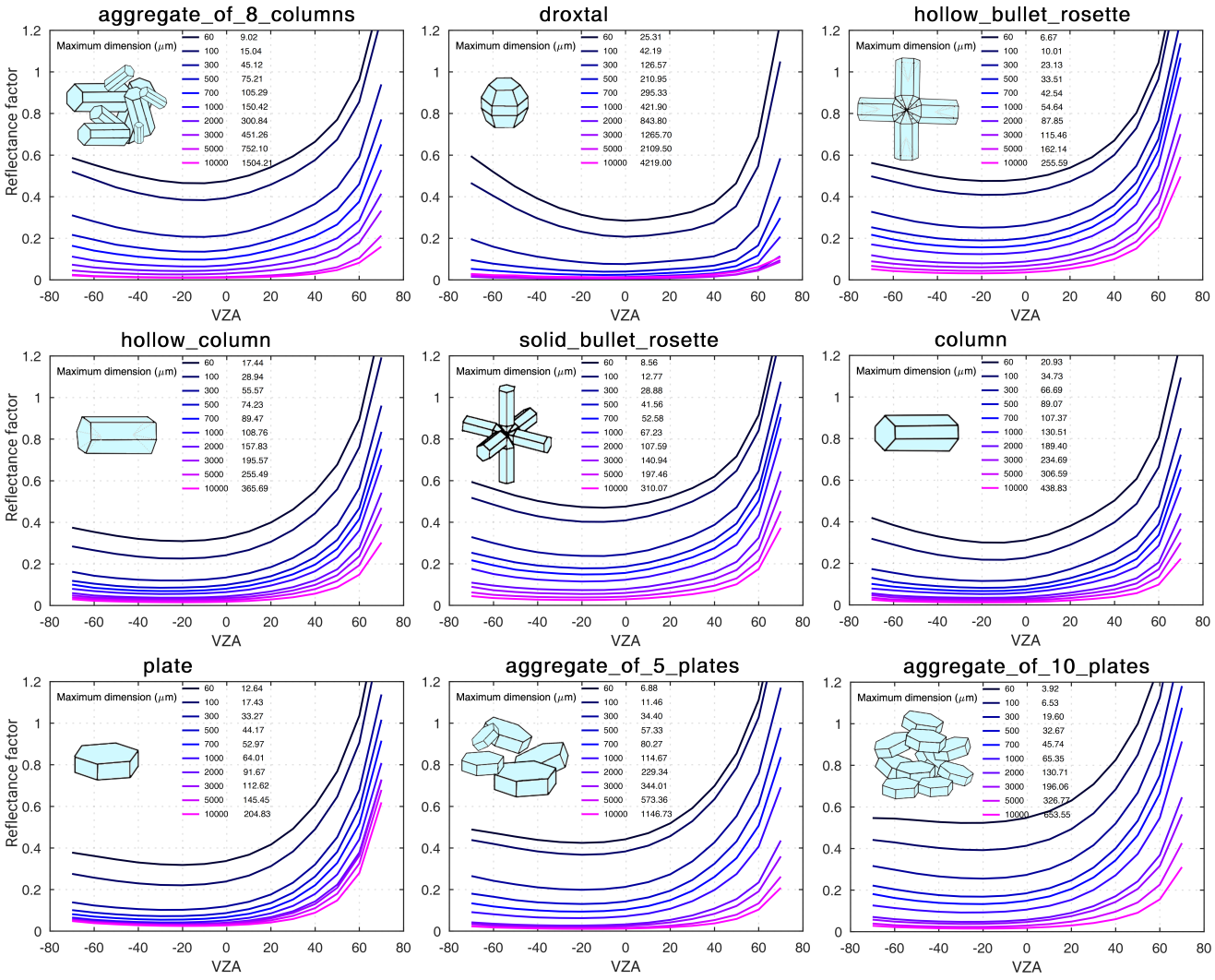

Specific comments:

#1 Comment to the Author

Abstract: (1) The first 1.5 paragraphs (L10-L19) are too general for an abstract. SCIATRAN is the first really specific information about the study presented in this

manuscript on Line 20. Please try to include specific information already earlier and leave some of the general motivation to the section 'Introduction'.

Author's response:

We modified the abstract and moved most of the first paragraph to introduction. We also brought key information about SCIATRAN to the beginning of abstract.

Modifications:

Line 1-11:

Accurate knowledge of the reflectance from snow/ice covered surface is of fundamental importance for the retrieval of snow parameters and atmospheric constituents from space-based and airborne observations. In this paper, we simulate the reflectance in a snow-atmosphere system using the phenomenological radiative transfer model SCIATRAN and compare the results with that of airborne measurements. To minimize the differences between measurements and simulation, we determine and employ the key atmospheric and surface parameters such as snow morphologies (or habits).

#2 Comment to the Author

L27: specify the used wavelength channels at this point.

Author's response:

Done.

Modifications:

Line 25-26:

…with that from airborne CAR measurements in the visible (0.670 µm) and NIR (0.870 and 1.6 µm) wavelength range.

#3 Comment to the Author

L31: round the effective radius to an integer number as the two decimals imply a precision which is not achievable.

Author's response:

Yes we agree, we rounded the numbers.

Modifications:

Line 30: ...an effective radius ~ 99

line 32: ...an effective radius ~ 83

#4 Comment to the Author

P2L41: please add the Arrhenius reference

Author's response:

Sorry we forgot it. We added the reference.

Modifications:

Line 44 and line 585:

Arrhenius, S., On the influence of carbonic acid in the air upon the temperature of the ground. Mag. J. Sci., London, Edinburgh, Dublin Phil, 41, 237-276, 1896.

#5 Comment to the Author

P5L129: It is very important to list the different atmospheric contributions to the measured radiance. However, please be a bit more precise in the formulation: for example, the scattering by the atmosphere before and after reaching the surface is not removed. More precisely, 'the contribution of light scattered by the atmosphere both before and after being reflected from the surface' is removed (see Schaepman-Strub et al., 2006). Please specify the four contributions accordingly, referring to the different contributions of scattered radiation reaching the instrument's field of view.

Author's response:

We modified the text accordingly.

Modifications: line 149 - 154

This removes the four atmospheric contributions from the measured radiance at TOA or flight altitude (Schaepman-Strub et al., 2006): the contribution of light scattered by the atmosphere: i) before the solar radiation has reached the surface, ii)after being reflected by the surface, iii) before and after reaching the surface and iv) the atmospheric path radiance.

#6 Comment to the Author

P5L134: please already give the CAR wavelength range at this point.

Author's response:

We added the wavelength range.

Modifications: line 157-158:

Sensitivity studies have demonstrated that atmospheric contributions to the CAR channel observations range from 3 to 12% depending on wavelength in the range of 0.381 to 2.324 µm.

#7 Comment to the Author

P5L138-149: This paragraph is very important to understand the quantities measured and simulated within this study. However, it is currently difficult to read. I recommend to reformulate the sentences and taking special care with regard to the sentence structure. This comment includes for example: P5L139: is applied to the measured radiances;

Author's response:

We corrected all paragraphs here and reformulated the sentences to transfer the message better.

Modifications: line 162-181

The atmospheric correction methods relies on different assumptions by which several source of uncertainties should be taken into account. In this study, to avoid such uncertainties, we do not apply an atmospheric correction to the measurements (radiances $L_{r,h}$) at flight altitude (h).. Instead, we calculate and use the reflectance at flight altitude by the following equation:

$$R = \frac{\pi L_{r,h}(\theta_i, \theta_r, \Delta\varphi)}{F_{0,\lambda} \cos\theta_i} \qquad (4)$$

where $L_{r,h}$ is the measured radiance at flight altitude. All reflectance/BRF_{λ}^{e} values at flight altitude in this study represent R in Eq. 4 and are referred to as “reflectance factor” in the snow-atmosphere system.

In the simulation of the reflectance factor in a coupled snow-atmosphere system, we need to account for atmospheric effects contribution properly. For this reason, we take independent data about atmospheric parameters (Aerosol Optical Thickness (AOT) and gases absorption) from ground-based and space-borne measurements. We select the data with the closest spatial and temporal interval actual airborne measurements. . We discuss more details of the atmospheric data and their application to the simulation routine in sect. 3 and 4. To estimate BRF_{λ}^{e} just above the surface, further atmospheric correction is needed. We assume the reflectance factor at flight altitude is a good estimation of BRF_{λ}^{e} just above the surface at infrared wavelengths where atmospheric scattering is negligible.

#8 Comment to the Author

P5L143: In the simulation […]: this sentence is unclear, please reformulate.

Author’s response:

Done.

Modifications: Line 172-175:

In the simulation of the reflectance factor in a coupled snow-atmosphere system, we need to account for atmospheric effects contribution properly. For this reason, we take independent data about atmospheric parameters (Aerosol Optical Thickness (AOT) and gases absorption) from ground-based and space-borne measurements.

#9 Comment to the Author

P5L147: We assume that the reflectance factor at flight altitude is a good approximation of the BRF just above the surface at infrared wavelengths where atmospheric scattering is negligible;

Author’s response:

We applied the change. The subscript 0 is defined in the Eq. 3.

Modifications: line 179-181:

We assume the reflectance factor at flight altitude is a good estimation of BRF_λ^e just above the surface at infrared wavelengths where atmospheric scattering is negligible.

Eq. 4: the subscript '0' should be defined at this point.

Author's response:

The subscript 0 is defined at line 130.

#10 Comment to the Author

Sect. 3: Subheadings would improve the readability considerably. I recommend to start with some more details about the ARCTAS spring campaign, adding a map with the flight tracks of the measurements used in this study, before giving details about the CAR instrument and the ozone and nitrogen dioxide data.

Author's response:

Thanks for pointing this out, yes it will definitely give a better introduction of the data we are using. We added a map of flight track and one paragraph about the campaign.

Modifications: line 186-191:

For this study, we used CAR data from the ARCTAS campaign conducted at Elson Lagoon, near Barrow/Utqiaġvik, Alaska, in April 2008 as part of the International Polar Year (Lyapustin et al., 2010; Gatebe and King, 2016). The goal of ARCTAS was to study physical and chemical processes in the Arctic atmosphere (e.g. long-range transport of pollution to the Arctic) and surface parameters (e.g. snow reflectance angular variation). The P-3B aircraft carried CAR instrument and was deployed by NASA from Fairbank. Fig. 1 shows the flight track on 7th of April 2008.

(We added figure 1).

Figure 1: Flight track of P-3B airplane carrying CAR on 07.04.2008 during ARCTAS campaign (Credit: NASA).

#11 Comment to the Author

Figure 1: please add the position of the Sun in the caption of the figure to make it immediately clear where the forward and backward scattering directions are.

Author's response:

We added the position of sun to the caption of Fig.2.

Modifications: line 772.

... solar zenith angle is 70.23°, 69.11° and 67.78° for flight altitude of 206, 647 and 1700 m respectively.

#12 Comment to the Author

Figure 2: missing whitespace before 1.649 um in the figure caption. The y axis should be named 'Reflectance factor', as this is what you calculate from Eq. 4.

Author's response:

Done. We corrected the caption and updated the figure.

Both Figure 1 and 2 should be described in more detail and not only mentioned in the text.

Author's response:

We explained detailed features of these two figures at lines 185-194. Perhaps it was not clear that our explanation is referring to these figures, so we made it clear.

Modifications: line 207-217:

Here is the explanation:

Examples of calculated reflectance factor values using Eq. (4) from CAR measurements on 7th of April, 2008 at Elson Lagoon (71.3° N, 156.4° W) are shown in Fig. 2 and Fig. 3. As we can see in these two figures, in spite of the influence of the atmospheric scattering and absorption, the general features of the snow BRF are clearly observable in polar plots as well as principal and cross plane plots: i) the decrease of snow reflectance with increasing wavelength due to the increasing absorption by snow at longer wavelengths; ii) the increase of the snow BRF as a function of VZA and the strong forward scattering peak in the principal plane at large VZA; iii) the smaller angular variation of the BRF at cross plane compared to the principal plane, though the reflectance values increase with VZA. The snow surface spatial inhomogeneity decreases with increasing altitude due to the change of spatial resolution with altitude (Gatebe and King, 2016; Lyapustin et al., 2010). Accordingly, at poorer spatial resolution, spatial homogeneity are more efficiently averaged as can be seen in Fig. 2 at flight altitude of 1700 m compared to 206 m in which we have higher spatial resolution.

#13 Comment to the Author

P6L173: You are giving an explanation for the decrease in inhomogeneities in the BRDF data. Please also discuss the increase of the BRF with altitude.

Author's response:

Sorry, it seems there was a misplacement of words. We should correct this sentence as following:

Modifications: line 213:

...the smaller angular variation of the BRF at cross plane compared to the principal plane, though the reflectance values increase with VZA.

#14 Comment to the Author

P6L182: In the paragraph describing the AOT data, a quick description of the representativeness of the aerosol conditions during the ARCTAS spring campaign with respect to the Barrow climatology would be helpful.

Author's response:

Thank you for reminding this point to us, yes its explanation will improve our introduction about the aerosol condition in this area. We added more information about the expected aerosol in Barrow.

Modifications: line 225-233:

Aerosol condition and its chemical and optical properties have been measured continuously at Barrow, Alaska, during different seasonal periods (Quinn et al., 2002). Previous studies indicate the largest contribution from sea salt, non-sea-salt sulfate and mineral dust. The average contribution of black carbon is very small compared to other aerosol types (Udisti et al., 2020). During the haze season (January to April), sea salt plays the dominant role in controlling light scattering in wintertime and non-sea salt sulfate in spring (Quinn et al., 2002). The increase on nss-sulfate in January to May is the long-range transport of anthropogenic primary nss sulfate besides the long-range transport of anthropogenic SO2 and its photo-oxidization to nss-sulfate with increase of light levels, and the local production of biogenic nss-sulfate.

In references:

Udisti, R., Traversi, R., Becagli, S., Tomasi, C., Mazzola, M., Lupi, A., and Quinn, P. K.: Arctic Aerosols in: Physics and Chemistry of the Arctic Atmosphere, edited by: Kokhanovsky, A. A., Tomasi, C., Springer Nature Switzerland AG, Cham, Switzerland, 2020.

Quinn, P. K., Miller, T. L., Bates, T. S., Ogren, J. A., Andrews, E., & Shaw, G. E.: A 3-year record of simultaneously measured aerosol chemical and optical properties at Barrow, Alaska., J. Geophys. Res., Atmos., 107(D11), AAC 8-1–AAC 8-15, 2002.

#15 Comment to the Author

P6L183: please provide some more details about the spaceborne measurements of total column ozone.

Author's response:

We added more details.

Modifications: line 236-238:

This data set (covering from 1995-present) consists of merged total ozone column data retrieved by WFDOAS from Global Ozone Monitoring Experiment (GOME), Scanning Imaging Absorption Spectrometer for Atmospheric Chartography (SCIAMACHY), and GOME-2A.

#16 Comment to the Author

P7L200: I guess the measurement location is sufficiently remote to justify this assumption. However, are there any measurements of black carbon on snow available for this region to further provide evidence for this?

Author's response:

Unfortunately, there was no measurement of the snow impurities such as black carbon collocated to the CAR measurements. Nevertheless, to understand the conditions at Barrow better and having a picture of existing aerosol there, we tried to collect information by looking at:

1) Long term continuous measurements of chemical and optical properties of aerosol at Barrow, Alaska (Kokhanovsky and Tomasi, 2020: chapter 4: Udisti et al., 2020): Based on 3 years continuous measurements, during the haze season (January to April), sea salt plays the dominant role in controlling light scattering in wintertime, and non-sea salt sulfate in spring. As can be seen from the Fig. A below, the average contribution of black carbon is very small compared to other aerosol types at Barrow.

2) Aeronet station at Barrow: Although from Aeronet we could not have information about the chemical composition of aerosol, the AOD values before old snow case (7th of April) does not show a significant episodic aerosol event by which snow could be polluted significantly. Our second case study (15th of April) is over fresh fallen snow in which the possibility of being affected by pollutants is even less.

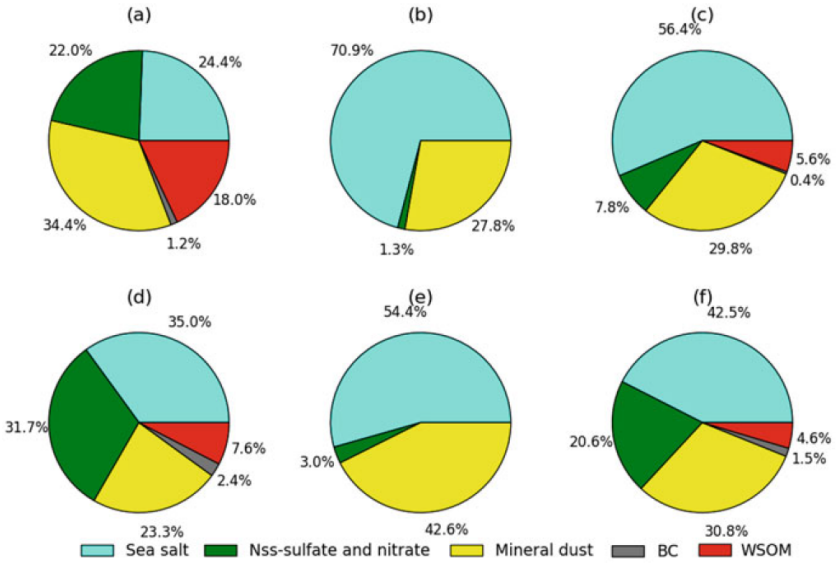

Fig. A: Average composition diagrams of the ground-level particulate matter sampled at Barrow during different seasonal periods. Summer time (June-September): (a), (b), (c): sub-micrometric, super micrometric and overall aerosol particles sampled; In winter time (October-May):(d), (e), (f): sub-micrometric, super-micrometric and overall aerosol particles sampled respectively. Different colours are used to indicate the main particulate matter constituents (sea salt, nss-sulfate and nitrate, mineral dust, black carbon (BC), and water-soluble organic matter (WSOM)

Modifications: line 225-233:

Aerosol condition and its chemical and optical properties have been measured continuously at Barrow, Alaska, during different seasonal periods (Quinn et al., 2002). Previous studies indicate the largest contribution from sea salt, non-sea-salt sulfate and mineral dust. The average contribution of black carbon is very small compared to other aerosol types (Udisti et al., 2020). During the haze season (January to April), sea salt plays the dominant role in controlling light scattering in wintertime and non-sea salt sulfate in spring (Quinn et al., 2002). The increase on nss-sulfate in January to May is the long-range transport of anthropogenic primary nss sulfate besides the long-range transport of anthropogenic SO2 and its photo-oxidization to nss-sulfate with increase of light levels, and the local production of biogenic nss-sulfate.

Udisti, R., Traversi, R., Becagli, S., Tomasi, C., Mazzola, M., Lupi, A., and Quinn, P. K.: Arctic Aerosols in: Physics and Chemistry of the Arctic Atmosphere, edited by: Kokhanovsky, A. A., Tomasi, C., Springer Nature Switzerland AG, Cham, Switzerland, 2020.

Quinn, P. K., Miller, T. L., Bates, T. S., Ogren, J. A., Andrews, E., & Shaw, G. E.: A 3-year record of simultaneously measured aerosol chemical and optical properties at Barrow, Alaska., J. Geophys. Res., Atmos., 107(D11), AAC 8-1–AAC 8-15, 2002.

#17 Comment to the Author

P8L229: please provide more details about the 'exponential vertical distribution' used for the vertical profile of the aerosol number density. Are you assuming the aerosol number density is reduced exponentially with height? Is this not influenced by the boundary layer height?

Author's response:

The reflectance of a surface-atmosphere system in spectral ranges without strong contribution of gaseous absorption depends mainly on AOT but not on the vertical distribution of aerosol number density. However, to perform radiative transfer calculations one need to assume some number density profile. The exponential profile was selected because it can be used as an approximation in the case of clean aerosol conditions. (see L. Mei, V. Rozanov, M. Vountas, J. P. Burrows, RC.Levy, W. Lotz, Retrieval of aerosol optical properties using MERIS observations: Algorithm and some first results, Remote Sensing of Environment, Volume 197, August 2017, Pages 125-140, for details).

And why were 3 km chosen when the measurements were conducted at flight altitudes below 1700 m?

Author's response:

The aerosol above flight altitude affects the downward solar radiation.

Also: for the vertical profiles of pressure and temperature, did you use monthly mean profiles as well or could you make use of radiosonde launches in the vicinity of the study area?

Author's response:

We took temperature and pressure profiles from the 2D chemical transport model: Sinnhuber B-M, Sheode N, Sinnhuber M, Chipperfield MP, Feng W , The contribution of

anthropogenic bromine emissions to past stratospheric ozone trends: a modelling study. Atmos Chem Phys 2009;9(8):2863–71.

Modifications: -

#18 Comment to the Author

Figure 3: (1) The ice crystal shapes presented in Figure 3 do not match the 9 morphologies introduced on P7L206: it seems you are presenting solid bullet rosettes in the figure, which are not mentioned in the text. On the other hand, you are not presenting the results for the fractal particles. Please clarify that as it is a bit confusing to me.

Author's response:

Sorry for the confusion. We added solid bollet rosette to text as well. Unfortunately, the database for solid bullet rosette was not fully ready in SCIATRAN. And we could not use it for effective radius retrieval. However, we could calculate and show the effect of its shape and size in Fig. 3.

Fractal is not shown in Fig.3, because in this figure, we focus on the new database of SCIATRAN and fractal was an old snow morphology. In addition, the range and existing size interval of fractal is completely different from the new database and ice crystals and we think having fractal in this figure will raise more confusion for the reader.

Modifications:-

#19 Comment to the Author

Figure 3: I assume this is still the calculated Reflectance factor, please name the y axis accordingly.

Author's response:

We corrected the label of Y axis accordingly. Now it is figure 4.

Modifications:

Please see figure 4.

#20 Comment to the Author

P9L264: please specify ‘same size’, as in the sentence before you are talking about a size range between 60 to 10000 um.

Author’s response:

We clarified this sentence.

Modifications: line 327-330

If we change only the shape of snow grain from “aggregate of 8 columns” to the “droxtal”, but we keep the size (largest dimension) as it is (e.g. 300 µm) this change provides a noticeable decrease of ~ 30% in reflectance at forward scattering direction for a viewing zenith angle of 60° and leads to a much weaker forward peak.

#21 Comment to the Author

P9L266: please clarify this sentence, because when I look at Figure 3, also for the plate shape the reflectance factor increases in the backward direction compared to the nadir direction.

Author’s response:

We clarified it. We meant in comparison to other shapes such as the aggregate of 8 column shape or droxtal.

Modifications: line 330-331

Noteworthy is, that the plate shape cannot reproduce the enhancement in backward direction (typical for a BRF over snow) as strong as the “aggregate of 8 columns” or the “droxtal" shape cause.

#22 Comment to the Author

P9L267: larger reflectance in all directions compared to what? The reflectance factor for the hollow bullet rosette seems to be at least equally high for some snow grain sizes compared to the aggregates of 5 or 10 plates.

Author’s response:

We corrected the sentence.

Modifications: line 332-333

Using the “aggregate of 5 and 10 plates” leads to larger reflectance in all directions compared to the single “plate” shape.

#23 Comment to the Author

Figure 4: (1) the green and blue lines and too similar and are hard to distinguish within the plot. (2) this is a reflectance factor again? Please name the y axis accordingly.

Author’s response:

Sorry for the color, we corrected it and changed the label of Y axis.

Modifications:

Please see the figure:

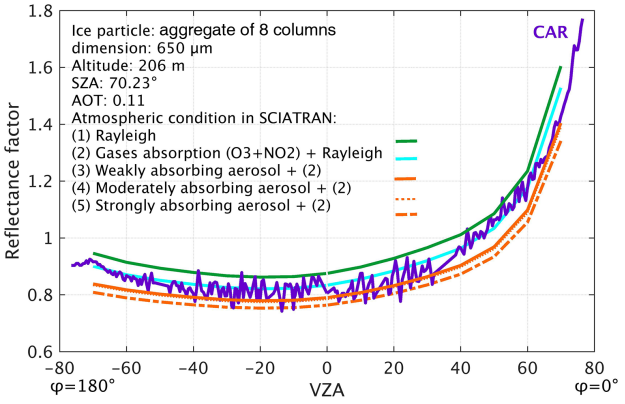

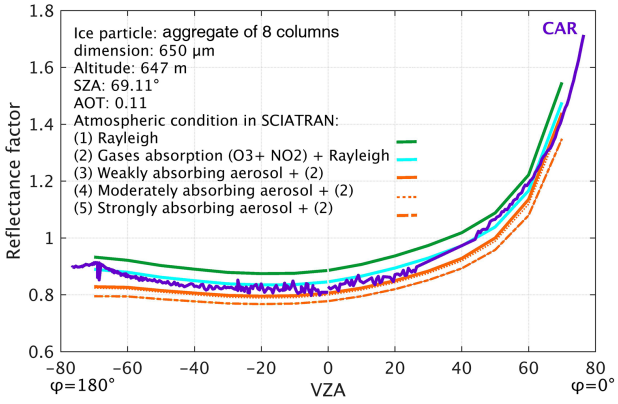

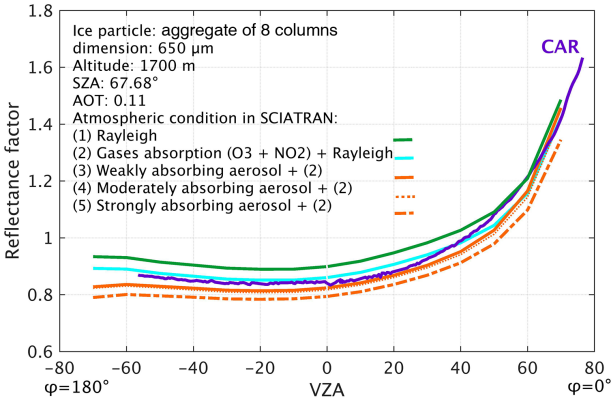

#24 Comment to the Author

Figures 5 and 6: (1) this is a reflectance factor again? Please name the y axis accordingly.

Author's response:

We corrected the Y axis label.

Modifications:

Please see Fig. 6 and 7.

#25 Comment to the Author

Figures 5 and 6: (2) The uncertainty of the CAR measurements needs to be included in the figure in the form of error bars. This also needs to be considered when calculating the RMSE. I assume a difference in RMSE of less than 0.4 % as visible between the chosen aggregates of 8 columns (98.8 um) and the columns (74.7 um) is not significant when considering possible measurement and retrieval uncertainties. This needs to be discussed in the manuscript.

Author's response:

We agree that uncertainty f measurements, simulation and retrieval are very important and should be plotted and discussed (as we explained in the beginning of comments). We added uncertainty envelopes to measurements in Fig. 5, 6 (now they are 6 and 7), which is 5% based on a comprehensive study done in NASA in 2007. We also provided this information in the text (as explained before).

Modifications:

Please see Fig. 6 and 7 and the text (line 385-387).

#26 Comment to the Author

The surface roughness clearly affects the CAR measurements at large viewing zenith angles. As I understand, the macroscopic surface roughness (in contrast to the ice crystal roughness) is not included in the SCIATRAN simulations?

In this case, I suspect you are trying to fit the simulations to the measurements using different single scattering properties for the different ice crystal shapes, while more

probably the macroscopic surface roughness is the underlying reason for the deviations between CAR measurements and SCIATRAN simulations. Macroscopic surface roughness enhances the backscatter by changing the effective angle of incidence, and reduces the forward scatter by casting shadows. Of course, this depends on the size of the roughness structures and their orientation, and I guess both parameters are unknown for the measurement conditions? Maybe some observations from within the aircraft with the naked eye or camera pictures could give an indication? At least the reduction in forward scattering of the CAR measurements compared to the simulations is visible for many different ice crystal shapes in Figure 5. Figure 6, however, shows an increase in the forward scattering as measured with CAR. In trying to choose the lowest RMSE for model simulations that neglect macroscopic surface roughness, it seems to me you can partly mimic the effect of surface roughness in choosing different ice crystal shapes (and single scattering properties). Thus, you are getting the 'right simulation', but for the wrong reasons in my point of view. Is there any way to test your simulations for different macroscopic surface roughness heights and orientation? Either way, this uncertainty needs to be discussed in detail within the manuscript.

Author's response:

Unfortunately, as you wrote macroscopic surface roughness is not included in the SCIATRAN. However, in Fig. 5 and 6, we are looking to 1.6 µm. We think at this wavelength, the effect of shadowing because of surface inhomogeneity is minimal. We do not think our effective radius retrieval and forward modeling for reflectance calculation at this spectral range is that much affected by surface roughness.

When we move to shorter wavelengths, such as 0.6 and 0.8 µm (Fig 8 and 9), we see the difference between measurement and simulation gets larger. We mentioned in the text that this larger difference can be due to surface roughness.

About the possible surface roughness in the measurement area, we know that we have sastrugi (with ~5cm height) in fresh snow case (we don't know about old snow), but no precise information about their orientation. But because of not modeling it in SCIATRAN, we could not estimate its effect unfortunately.

Modifications: -

#27 Comment to the Author

P11L333-345: The justification of the ice crystal shape retrievals with the temperature dependence seems dubious to me. One needs to be careful in differentiating the important temperatures here. It is true that temperature (and supersaturation!) strongly affect the shape of pristine ice crystals when the precipitating snow is formed within the cloud. If anything, the ice crystal shape should be connected to the temperature profile at the time of the last snowfall (excluding snow aging processes). However, the temperatures you are stating are temperatures measured in-flight, probably days after the precipitation event. This temperature is completely unrelated to the snow on the ground, especially as you report yourself that the snow surface consists of old snow during most days. After the snow has fallen to the ground, the vertical temperature gradient at the surface and within the snowpack is way more important for the ice crystal shape (influencing snow metamorphism processes). If you don't have in situ observations looking at the ice crystal shape on the ground, you cannot validate your ice crystal shape retrieval in that way.

Author's response:

We agree that temperature and super-saturation effect needs more investigation, which was not in the scope of our manuscript. However, we mentioned a few sentences about the possible relation between snow morphology and the temperature to highlight that there is a room for investigation. Though, we did not use temperature argument to validate our findings about snow morphology, we understand your point, we should not bring it in the abstract and so we delete it from abstract because it's not a confirmed finding of our work.

But we kept a few sentences in the discussion part. And we added your point that one needs to be careful about temperature and emphasized that more investigation is needed.

We think the temperature is representative enough for fresh snow case but we agree that for old snow case, the temperature at the time of snowfall is also important. We added your point to the paper.

If you think it's fine to keep it after the mentioned modification in the manuscript we would do so, if not, we will delete it.

Modifications: line 407-413:

Though the real nature of ice crystal shape at the time of measurement is not known to us, the impact of temperature and supersaturation on morphology of snow grain particles has been debated in previous studies. (Slater and Michaelides, 2019; Shultz, 2018; Libbrecht, 2007; Bailey and Hallett, 2004; Yang et al., 2003). Based on the relationship between temperature and snow grain morphology, the column-based shapes are the dominant ice crystal morphology in environments with temperatures higher than -10°C whereas plates are dominant if the temperature is less than -10°C. Though, more investigation is needed especially to account for the temperature profile at the exact time of snowfall, our findings with respect to the most representative shape for each case study agree with this argument. The temperature range during CAR measurements at 6-7th of April 2008 is from -20 to -5°C. Based on our results the "aggregate of 8 columns" is the most representative shape for measurements conducted on this day. On 15th of April 2008 when the temperature range changes to -23 to -17°C, mainly plate-based ice crystal shapes are expected for such low temperatures and our results confirm this argument.

#28 Comment to the Author

Figure 7: This is way more illustrative and provides more information than Table 2, which becomes redundant in my point of view and can be removed from the manuscript.

Author's response:

Referee Nr. 1 asked us to add asymmetry parameter to table 2 (now is table 3). So we still tend to keep it if it is fine. Please let us know if you think we should remove it.

Modifications:-

#29 Comment to the Author

P12L359: it seems you are normalizing the RMSE somehow. Please provide the formula how you calculated the RMSE, as your description in the text seems to be imprecise.

Author's response:

To calculate RMSE:

$$RMSE=\sqrt{\frac{1}{n}\sum_{i=1}^{n}\left(\frac{x_{obs}-x_{simulation}}{x_{obs}}\right)^2}\times 100$$

Modifications:-

#30 Comment to the Author

P12L364: please round the effective radii to integer values. Providing two decimals is implying a degree of accuracy which is not achieved.

Author's response:

done.

Modifications: line 447-448

...with a maximum dimension of 650 μm (effective radius 99 μm) for the case of old snow, and "aggregate of 5 plates" ice crystals with a maximum dimension of 725 μm (effective radius 83 μm) for the case of fresh snow.

#31 Comment to the Author

Figure 8: caption: 'reflectance factor'

Author's response:

Done.

Modifications: caption of Fig . 9:

Left column shows reflectance factor at three wavelengths:…

#32 Comment to the Author

P12L367: I would recommend introducing Figure 10 only after Figures 8 and 9.

Author's response:

We moved the introduction of this figure to after Figure 8 and 9.

Modifications: line 452-461:

In Fig. 9, the difference between the simulated and measured reflectance factor at 0.677 and 1.649 μm is small on average, being less than 0.025 in regions of small VZA and not

exceeding ±0.05 for larger VZA < 50°. These values are larger at 0.873 µm; the maximum difference reaches ~ ±0.05 for small VZA. The difference between SCIATRAN simulation values and those of the measurements is pronounced in the forward scattering region where $|\Delta\varphi| < 40°$. Fig. 10 is the same plot as Fig. 9 but for fresh snow. The differences between SCIATRAN simulations and CAR measurements of the reflectance factor are less pronounced in the glint region, as compared to those for the old snow.

To assess the accuracy of simulations over all azimuth angles, the correlation plot and the Pearson correlation coefficient between measured and modelled reflectance factor are shown in Fig. 11. As it is shown in ...

#33 Comment to the Author

Figure 10: (1) caption: 'reflectance factor', x and y axis: 'reflectance factor', please state again in the caption which columns belong to the old and new snow cases.

Author's response:

Done.

Modifications: Figure 11 and caption:

Caption: The scatter plot with corresponding pearson correlation coefficient of reflectance factor measured by CAR and simulated by SCIATRAN; left column shows he results for old snow, right column: fresh snow. Here the color bar represents number density of pixels.

#34 Comment to the Author

I am interested in seeing a comparison of the correlation coefficients between new snow case and the lowest flight level of the old snow case as they have roughly comparable flight altitudes. This might make it easier to discuss a possible influence of surface inhomogeneities. At this point it would also help to provide more details about the differences in flight tracks between the two measurement days. Was the same area probed on both days? Otherwise of course, even the same flight altitude might not be

comparable. This is connected to my earlier comment to provide more details about the actual flights performed during the campaign.

Author's response:

Unfortunately, the case of fresh and old snow in our study are not exactly over the same area (We have the coordinates of flight path and measurement). Actually, we were very much interested to see this comparison to understand more about the effect of surface inhomogeneity. Nevertheless, we were not able to do so because they are not comparable.

Modifications: -

#35 Comment to the Author

P12L377: I do not agree with the conclusion drawn here. The high correlation coefficient and small discrepancies do not justify the selection of this wavelength channel for the selection of the best ice crystal shape. The correlation coefficient and small bias is made 'by construction', as you selected the ice crystal shape based on the lowest bias between simulation and CAR measurements in the first place. The high correlation coefficients for this wavelength channel are therefore not surprising.

Author's response:

We agree, and deleted this sentence.

Modifications: line 468.

#36 Comment to the Author

The last sentence of this section (P12L379) seems a bit out of place and should be rephrased.

Author's response:

Sorry this sentence should move to previous paragraph in which we compare polar plots. It was misplaced during several modifications of our paper.

Modifications: moved from line 470 to line 456.

Please see text.

#37 Comment to the Author

P13L388: This is an important point and should be included in this study already by looking at the correlation coefficient between measured and simulated reflectance factors and their dependence on the flight altitude for the case of old snow. I am interested to see whether there is a clear dependence of the correlation coefficient on the flight altitude.

Author's response:

We calculated the correlation coefficient for Fig. 5 which is a comparison of reflectance at different altitudes at 0.67µm, principal plane. The correlations gets higher when we move from ~200 m to 600 m. But there wasn't an increase when we move from 600m altitude to 1700m.

Modifications:-

#38 Comment to the Author

P13L405: With regard to my earlier comment, the justification of the ice crystal shape retrieval with the temperature dependence cannot be mentioned here (and also not in the abstract).

Author's response:

We explained in previous comment that we did not use temperature argument to validate our findings. The aim of mentioning this relation between snow morphology and temperature was more to highlight that there is room to investigate the possible relation. But we understand your point, we deleted this argument from abstract (as it needs more investigation and it's better not to represent it in the abstract). But we kept a few sentences in discussion part. And we added your point that one needs to be careful about temperature and emphasized that more investigation is needed.

If you think it's fine to keep it after the mentioned modification in the manuscript we would do so, if not, we will delete it.

Modifications: line 407-413:

Though the real nature of ice crystal shape at the time of measurement is not known to us, the impact of temperature and supersaturation on morphology of snow grain particles has been debated in previous studies. (Slater and Michaelides, 2019; Shultz, 2018; Libbrecht, 2007; Bailey and Hallett, 2004; Yang et al., 2003). Based on the relationship between temperature and snow grain morphology, the column-based shapes are the dominant ice crystal morphology in environments with temperatures higher than -10°C whereas plates are dominant if the temperature is less than -10°C. Though, more investigation is needed especially to account for the temperature profile at the exact time of snowfall, our findings with respect to the most representative shape for each case study agree with this argument. The temperature range during CAR measurements at 6-7th of April 2008 is from -20 to -5°C. Based on our results the "aggregate of 8 columns" is the most representative shape for measurements conducted on this day. On 15th of April 2008 when the temperature range changes to -23 to -17°C, mainly plate-based ice crystal shapes are expected for such low temperatures and our results confirm this argument.

#39 Comment to the Author

P13L416: I wonder why the use of a vertically inhomogeneous snow layer in the model is only mentioned here and not in the discussion of the results already. It should not be mentioned for the first time in the Conclusions in my point of view.

Author's response:

Assuming vertically inhomogeneous snow layer and investigating its effect was not in the scope of our work and we mentioned it only in the conclusion as a room to improve and consider in future works. That is why we did not mention this in the discussion of results. We hope it's fine to keep it as it is because we do not have enough information to present about it in the discussion section.

Modifications: -

Technical corrections

#1 Comment to the Author

P1L30: Assuming that the snow layer consists […]

Author's response: Done.

Modifications: line 29: Assuming that the snow layer consists […]

#2 Comment to the Author

P3L78: delete ';' after '2011'

Author's response: Done.

Modifications: line 92...Kokhanovsky, 2011).

#3 Comment to the Author

P3L88: 'phenomenological', 'airborne'

Author's response: Done.

Modifications: line 103-104...well validated phenomenological RTM, and the airborne observations...

#4 Comment to the Author

P5L126: of the surface

Author's response: Done.

Modifications: line 147: To isolate the reflectance properties of the surface...

#5 Comment to the Author

P5L127: on the measured radiance

Author's response: Done.

Modifications: line 148:...correction methods on the measured radiance at TOA...

#6 Comment to the Author

P5L128: scattering or absorption applying RTMs

Author's response: Done.

Modifications: line 149:...scattering or absorption applying RTMs...

#7 Comment to the Author

P5L128: This removes the four atmospheric [...] from the measured radiance: i) [...]

Author's response: Done.

Modifications: line 149: This removes the four atmospheric contributions from the measured radiance at TOA or flight altitude:...

#8 Comment to the Author

P5L153: delete 'etc' or be more specific

Author's response: Done.

Modifications: line 184:...up to present to measure the single scattering albedo of clouds, the bidirectional reflectance of various surface types and acquiring imagery of clouds and the Earth's surface.

#9 Comment to the Author

P6L160: by a mirror – missing blank

Author's response: Done.

Modifications: line 197: CAR collects data by a mirror rotating 360° in a plane perpendicular...

#10 Comment to the Author

P6L163: do you mean viewing zenith and azimuth angles?

Author's response: Yes, thanks, done.

Modifications: line 199:...both viewing zenith and azimuth angles...

#11 Comment to the Author

P6L163: Please rephrase: The high [...] resolution [...] allows the estimation of the anisotropy of the reflectance in the snow-atmosphere system with high accuracy.

Author's response: Thanks, done.

Modifications: line 199: The high angular/spatial resolution of 1° in both viewing zenith and azimuth angles allows the estimation of the anisotropy of the reflectance in the snow-atmosphere system with high accuracy.

#12 Comment to the Author

P6L167: RTM simulations

Author's response: Done.

Modifications: line 206:...atmospheric effects in RTM simulations.

#13 Comment to the Author

P6L175: do you mean spatial inhomogeneity?

Author's response: Yes. Done.

Modifications: line 214: The snow surface spatial inhomogeneity decreases...

#14 Comment to the Author

P7L208: eight ice crystal shapes/habits

Author's response: Done.

Modifications: line 259: Recently, a new data library of basic single scattering properties of eight ice crystal shapes/habits developed by...

#15 Comment to the Author

P7L208: (referred to as fractal in this paper)

Author's response: Done.

Modifications: line 266: Koch fractal (referred to as fractal in this paper) particles are used as well

---

#16 Comment to the Author

P8L227: ground-based measurements from AERONET

Author's response: Done.

Modifications: line 286: Using AOT from ground-based measurements of AERONET...

#17 Comment to the Author

P8L228: selecting one of the aerosol types

Author's response: Done.

Modifications: line 287:...as mentioned and selecting one of the aerosol types...

#18 Comment to the Author

P9L271: a priori knowledge

Author's response: Done.

Modifications: line 338: ... highlights the importance of having accurate a priori knowledge or estimation of size of the ice crystals and their shapes to simulate accurately measurements.

#19 Comment to the Author

P9L272: to accurately reproduce measurements

Author's response: Done.

Modifications: line 339:... a priori knowledge or estimation of size of the ice crystals and their shapes to accurately reproduce measurements.

#20 Comment to the Author

P9L279: evaluate the impact of the atmosphere

Author's response: Done.

Modifications: line 349: Therefore, in this section, absorption bands e.g. 0.677 µm are selected to evaluate the impact of the atmosphere.

#21 Comment to the Author

P9L282: assuming the following properties

Author's response: Done.

Modifications: line 352: The calculations are performed assuming the following properties of the atmosphere and snow layer:...

#22 Comment to the Author

P12L362: described in the previous sections

Author's response: Done.

Modifications: line 445: The simulations, which used the results and findings described in the previous section were performed…

#23 Comment to the Author

P12L380: measurement of the reflectance factor

Author's response: Done.

Modifications: line 458: The differences between SCIATRAN simulations and CAR measurements of the reflectance factor are less pronounced…

#24 Comment to the Author

P13L390: reflectance factor

Author's response: Done

Modifications: line 482: The SCIATRAN RTM (a phenomenological RTM) was used to simulate the reflectance factor in the snow-atmosphere…

#25 Comment to the Author

P13L397: reflectance factor

Author's response: Done.

Modifications: line 489, In our case study at Barrow/Utqiaġvik, the simulated reflectance factor assuming…

#26 Comment to the Author

P13L408: reflectance factor

Author's response: Done.

Modifications: line 501: In our study, the simulated patterns of the reflectance factor with respect to spectral and directional signatures produce well the measurements...

#27 Comment to the Author

P13L411: reflectance factor

Author's response: Done.

Modifications: line 505... the overall absolute difference between the modeled reflectance factor from SCIATRAN and CAR...

#28 Comment to the Author

P14L429: comma misplaced

Author's response: Done.

Modifications: line 526... respectively.

#29 Comment to the Author

P15L466: do you really mean TOA reflectance? Or reflectance at flight altitude?

Author's response: Thanks for pointing it out, we should say reflectance at flight altitude. Done.

Modifications: Line 566: The calculation of weighting functions and reflectance at flight altitude is performed at each iteration step using the radiative transfer model SCIATRAN (Rozanov et al., 2014).

~~On the retrieval of snow grain morphology, the accuracy of~~ Ssimulated reflectance aboveover snow, constrained byusing airborne measurements of solar radiation ~~in the Arctic~~: Implications for the snow grain morphology in the Arctic

Soheila Jafariserajehlou[1], Vladimir V. Rozanov[1], Marco Vountas[1], Charles K. Gatebe[2,3] and John P. Burrows[1]

[1]Institute of Environmental Physics, University of Bremen, Bremen, Germany
[2] Universities Space Research Association (USRA), Columbia, MD, USA
[3] NASA Goddard Space Flight Center, Greenbelt, MD, USA

Correspondence to: Soheila Jafariserajehlou (jafari@iup.physik.uni-bremen.de)

Abstract. Accurate knowledge of the reflectance from snow/ice covered surface is of fundamental importance for the ~~investigation and~~ retrieval of snow parameters and atmospheric constituents from space-based and airborne ~~passive remote sensing~~ observations. ~~This is a prerequisite for identifying and quantifying changes in the environment and climate in Polar Regions. However, the current differences between simulated and measured reflectance in a coupled snow-atmosphere system, leads to systematic errors in the determination of the amount of trace gases, aerosol and cloud parameters from space based and airborne passive remote sensing observations~~.

In this paper, we simulate the reflectance in a snow-atmosphere system using the phenomenological radiative transfer model SCIATRAN and compare the results with that of airborne measurements. To minimize the differences between measurements and simulation, ~~The goal of our study is to~~we determine and employ the key atmospheric and surface parameters such as snow morphologies (or habits) ~~to minimize the differences between measurements and simulation~~, ~~describe studies of the retrieval of snow grain morphologies, also called habits, and their use to determine reflectance and test the accuracy of our radiative transfer model simulations of reflectance by comparison with measurements~~. Firstly, we report on a sensitivity study. This addresses the requirement for adequate a priori knowledge about snow models and ancillary information about the atmosphere; the objective being to minimize differences between measurements and simulation. For this aim, we use the well-validated phenomenological radiative transfer model SCIATRAN. Secondly, ~~and more importantly~~, we present and apply a ~~novel~~ two-stage snow grain morphology (i.e. size and shape of ice crystals in the snow) retrieval algorithm. We then describe the use of this new retrieval to estimate the most

representative snow model, using different types of snow morphologies, for the airborne observation conditions, performed by NASA's Cloud Absorption Radiometer (CAR). ~~The results show that the retrieved ice crystal shapes are consistent with the expected snow morphology (estimated from temperature information) in the measurement area over Barrow/Utqiaġvik, Alaska in 2008.~~

Thirdly, we present a comprehensive comparison of the simulated reflectance (using retrieved snow grain size and shape as well as independent atmospheric data) with that from airborne CAR measurements in the visible (0.670 µm) and NIR (0.870 and 1.6 µm) wavelength range. The results of this comparison are used to assess the quality and accuracy of the radiative transfer model in the simulation of the reflectance in a coupled snow-atmosphere system.

Assuming that that the snow layer consists of ice crystals with "aggregates of 8 column" ice habit, having an effective radius ~ 9998~~.83~~ µm, we find that for a surface covered by old snow, the Pearson correlation coefficient, R, between measurements and simulations is ~~to be~~ 0.98 (R^2 ~ 0.96). For freshly fallen snow, assuming that snow layer consists of the "aggregate of 5 plate" ice habit with effective radius ~ 83 µm and ~~on areas~~ having surface inhomogenity, the correlation is ~ 0.97 (R^2 ~ 0.94) in the infrared and 0.88 (R^2 ~ 0.77) in the visible wavelengths~~, assuming that snow layer consists of aggregate of 5 plate ice habit with effective radius ~ 83.41 µm~~. Largest differences between simulated and measured values are observed in the glint area~~,~~ (i.e. in the angular regions of specular and near-specular reflection), with relative azimuth angles <± 40° in forward scattering direction. The absolute difference between the modeled results and measurements in off-glint regions with viewing zenith angle less than 50° is generally small ~ ±0.025 and does not exceed ±0.05. These results will help to improve the calculation of snow surface reflectance and relevant assumptions in the snow-atmosphere system algorithms ~~designed to retrieve atmospheric parameters such as~~ (e.g. aerosol optical thickness retrieval algorithms in the Polar Regions).

1 Introduction

The extent and type of snow and ice cover have a significant impact on climate, as noted by Arrhenius over 100 years ago (Arrhenius, 1896). There is a positive feedback between decreasing surface temperature, an increase of snow and ice cover and an associated increase in planetary albedo, which then further decreases surface temperature and vice versa. Consequently, changes in snow and ice extent and morphology play a key role in climate change, ~~and h~~ Having accurate knowledge about snow/ice covered surface~~it~~, is a prerequisite for identifying and quantifying changes in the climate. ~~(~~Schneider and Dickinson, 1974; Curry et al., 1995; Cohen

et al., 2014; Kim et al., 2017; Wendisch et al., 2017; 2019). ~~Therefore having accurate knowledge about it is a prerequisite for identifying and quantifying changes in the climate.~~

In addition, ~~D~~during the past recent decades the Arctic region has warmed more rapidly than other regions. This phenomenon is known as the Arctic Amplification (AA) (Serreze and Barry, 2011). The analysis of the growing number of long-term records of the data products (e.g. the amount of trace gases, aerosol and cloud parameters), retrieved from passive and active satellite observations, provides potentially invaluable information to identify and quantify the evolution and consequences of AA (Wendisch et al., 2017).

Because of the magnitude of the scattering from snow, the use of remote sensing measurements above snow covered surfaces in the cryosphere, requires accurate models of the scattering and reflectance from snow surfaces. However, the current differences between simulated and measured reflectance in a coupled snow-atmosphere system, lead to systematic errors in the determination of the ~~to retrieve information about~~ atmospheric constituents in particular clouds and aerosol parameters but also trace gases ~~and avoid systematic errors~~ (e.g. Istomina et al., 2010; 2012; Jafariserajehlou et al., 2019).

A large number of experimental and theoretical studies have been conducted measuring and modeling snow optical properties such as the angular distribution of reflected light over and within the snow surface and the subsequent derivation of snow albedo. The early measurements by Middleton and Mungal (1952) and the model of Dunkle and Bevans (1956) used to analyze the transmittance and reflectance of snow cover were the beginning of considerable efforts on this topic. Barkstrom (1972) formulated and solved the scattering problem for snow surfaces in terms of radiative transfer theory. Later, the comparison of reflectance from snow-covered surfaces simulated by Radiative Transfer Models (RTM) with that of observation made substantial progress in ~~our~~ our understanding of the angular distribution of ~~snow~~ reflectance above snow surface. ~~has been made by comparing the simulated reflectance from snow covered surfaces simulatedcalculated by Radiative Transfer Models (RTM) with that of observations~~ (e.g. Wiscombe and Warren 1980; Warren et al., 1998; Arnold et al., 2002; Painter and Dozier, 2003; Kokhanovsky and Zege, 2004; Li and Zhou, 2004; Hudson et al., 2006; Hudson and Warren, 2007; Lyapustin et al., 2010; Kokhanovsky and Breon, 2012).

The reflection/scattering patterns of snow-covered surface can be summarized as follows: i) snow is not a Lambertian reflector in the visible and near infrared spectral region; its reflectance has anisotropic nature and the anisotropy increases with wavelength; ii) unlike other surface types (e.g. vegetation or soil) with a strong peak in back-scattering~~backscattering~~ direction (the hot spot effect), snow has a strong forward peak for large viewing zenith angles (e.g. Gatebe and King, 2016); iii) The snow reflectance variation is larger in the principal plane~~,~~ (i.e. the plane containing the Sun, surface normal and observation direction), than in the cross plane~~,~~ (i.e.

the one perpendicular to principal plane) (Warren, 1982; Lyapustin et al., 2010; Kokhanovsky and Breon, 2012). However, the remaining discrepancies between simulated reflectance in a snow-atmosphere system results and field measurements led to further investigations in the field of single scattering properties of snow grains (Mishchenko et al., 1999; Jin et al., 2008, Yang et al., 1998; 2003; 2013), surface roughness (Warren et al., 1998; Hudson et al., 2006; Hudson and Warren, 2007; Lyapustin et al., 2010; Zhuravleva and Kokhanovsky, 2011) and atmospheric correction methods (Lyapustin et al., 2010). Despite substantial improvements, the uncertainties in our understanding of the microphysical and macroscopic properties of snow are an unresolved issue for RTMs, ray-tracing and climate models. For example, the current state of the art RTMs yield much more anisotropic reflectance behavior for snow in the glint region than observed in reality (Zhuravleva and Kokhanovsky, 2011; Lyapustin et al., 2010; Hudson and Warren, 2007; Warren et al., 1998). These studies either focus on the snow reflectance at the surface, employing an atmospheric correction method (Leroux et al., 1998; Kokhanovsky and Zege, 2004; Kokhanovsky et al., 2005; Lyapustin et al., 2010; Negi and Kokhanovsky, 2011;) or consider the atmospheric effects without in-depth investigations of the surface parameters (Aoki et al., 1999; Hudson et al., 2006; Kokhanovsky and Breon, 2012). A comprehensive study and investigation of both snow layer and atmosphere parameters in a coupled snow-atmosphere system has not yet been undertaken but is required to improve the accuracy of remote sensing retrieval algorithms for aerosol and cloud in the Arctic region (Istomina et al., 2010; 2012; Jafariserajehlou et al., 2019).

Consequently, tThe intentgoal of this paperstudy is to: i) study the sensitivity of scattering and reflectance in the coupled snow-atmosphere system totaking into account both surface and atmospheric parameters; ii) retrieve the most representative ice crystal morphology by applying a snow grain size and shape retrieval algorithm to measured reflectance at the wavelength of 1.6 µm; iii) evaluate the ability of a phenomenological RTM, to reproduce the measured reflectance over the spectral range 0.34 µm - 1.649 µm at all available observation directions using the retrieved atmospheric and snow parameters.

In this study, we use Tthe RTM SCIATRAN (Rozanov et al., 2014) which is a well validated phenomenological RTM, and the airborne observations of reflectancethe scattered and reflected solar radiation, acquired by Cloud Absorption Radiometer (CAR) were used in this study. The CAR measurements were made during the Arctic Research of the Composition of the Troposphere from Aircraft and Satellite (ARCTAS) spring 2008 campaign over Barrow/Utqiaġvik, Alaska, in 2008. Further The information about the atmospheric parameters during the ARCTAS campaign measurement campaign of the CAR instrument was taken from available AERONET and satellite data.

The ~~rest of this~~ paper is organized as follows: ~~comprises the following. I~~in the next ~~section~~section, we present the theoretical background and terminology used to calculate the angular distribution of reflectance in a snow-atmosphere system. In sect. 3 and 4, we introduce and explain the measurements and the simulation methods. ~~are introduced and explained.~~ In sect. ~~5~~5, the sensitivity of reflectance to the underlying snow layer and atmospheric parameters is~~are~~ investigated. In sect. 6, the results of applying the two-stage snow grain size and shape retrieval algorithm are presented. In sect. 7, the results of the reflectance simulations are compared to CAR measurements. Finally, conclusions are drawn in sect. 8. Appendix contains detailed description of the snow grain size and shape retrieval algorithm used in the study.

2 Theoretical background

To describe the directional signature of reflectance over different surface types, the Bidirectional Reflectance Distribution Function (BRDF) as defined by Nicodemus (1965), is the commonly used reflectance quantity. The term BRDF describes the reflection of incident solar radiation from one direction to another direction (Nicodemus 1965). The mathematical form of BRDF is expressed as (Nicodemus et al., 1977; Schaepman-Strub et al., 2006):

$$BRDF_{\lambda}=\frac{d\,L_r(\theta_i,\varphi_i,\theta_r,\varphi_r;\lambda)}{d\,E_i(\theta_i,\varphi_i;\lambda)}\left[sr^{-1}\right], \qquad (1)$$

where L_r is the reflected radiance, θ and φ are the zenith and azimuth angles, respectively. The subscript i corresponds to the incident and r to the reflected beams. E is the incident surface flux (irradiance) and λ is the wavelength. However, the BRDF is not a directly measurable quantity because of its being formulated as a ratio of infinitesimal quantities (Nicodemus et al., 1977; Schaepman-Strub et al., 2006). Nicodemus et al. (1977) provided an extensive description of reflectance terminologies and measurable quantities e.g. the Bidirectional Reflectance Factor (BRF), the Hemispherical Directional Reflectance Factor (HDRF), the Directional Hemispherical reflectance (DHR), etc. According to Nicodemus et al. (1977) and Schaepman-Strub et al. (2006) each of the terms is defined for the specific illumination and reflectance geometries for which, the reflectance properties are measured (e.g. satellite, airborne or laboratory measurement conditions). Following the method of Gatebe and King (2016), the effective BRDF at a horizontal (flat) reference plane is defined as:

$$BRDF^{e}_{\lambda}=\frac{\Delta L_r(\theta_i,\varphi_i,\theta_r,\varphi_r;\lambda)}{\Delta E_i(\theta_i,\varphi_i;\lambda)}=\frac{\Delta L_r(\theta_i,\varphi_i,\theta_r,\varphi_r;\lambda)}{\Delta L_i(\theta_i,\varphi_i;\lambda)\cos\theta_i\Delta\omega_i}\left[sr^{-1}\right], \qquad (2)$$

where $BRDF^e_\lambda$ is as an average of the BRDF over an appropriate area, angle and solid angle for specific observation geometry; $\Delta\omega_i$ is a finite solid angle element. The validity of this approximation relies on the experimental evidence that the BRDF is not significantly influenced by the following effects: the finite intervals of area, angle, solid angle and the distribution function; sub-surface scattering; radiation parameters such as wavelength and polarization, fluorescence etc. (i.e. significant variations do not occur within small intervals, see Nicodemus et al., 1977; Gatebe and King, 2016). As a result, the $BRDF^e_\lambda$ is determined by:

$$BRDF^e_\lambda = \frac{L^e_r(\theta_i, \theta_r, \Delta\varphi)}{F_{0,\lambda}\cos\theta_i}, \quad (3)$$

where L^e_r is the measured radiance, $F_{0,\lambda}$ is the solar irradiance incident at the top of atmosphere (TOA). Often, it is helpful to have a description of the difference between the measured surface reflectance and a Lambertian reflector; in such a case the equivalent Bidirectional Reflectance Factor BRF^e_λ, which is $BRDF^e_\lambda$ multiplied by π is more representative.

To isolate the reflectance properties of the surface and derive BRF^e_λ or $BRDF^e_\lambda$ just above the surface, we need to apply atmospheric correction methods on the measured radiance at TOA or flight altitude (e.g. by using knowledge of the atmospheric scattering or absorption applying ~~using~~ RTMs). This removes the four atmospheric contributions from the measured radiance ~~, the four atmospheric contributions from the atmosphere~~ at TOA or flight altitude (Schaepman-Strub et al., 2006): the contribution of light scattered by the atmosphere~~: i) the atmospheric path radiance, ii) the scattering by the atmosphere~~ i) before the solar radiation has reached the surface, ~~iii) the scattering by the atmosphere~~ ii)after being reflected by the surface, ~~iv) the scattering by the atmosphere~~ iii) before and after reaching the surface and iv) the atmospheric path radiance.

However, most of the atmospheric contributions in measurements close to the surface are negligible (except diffuse component ~~-~~number ii) and measured quantities represent the "at surface" radiance (Schaepman-Strub et al., 2006). Sensitivity studies have demonstrated that atmospheric contributions to the CAR channel observations range from 3 to 12% depending on wavelength in the range of 0.381 to 2.324 µm (Soulen et al., 2000). Consequently, previous studies presented either the BRFs in a surface-atmosphere system at flight altitude without atmospheric correction (Soulen et al., 2000) or the BRFs right above the surface after atmospheric correction (Gatebe et al., 2005; Gatebe and King 2016).

The atmospheric correction methods relies on different assumptions by which several source of uncertainties should be taken into account. In this study, to avoid such uncertainties ~~arising from different assumptions being~~

~~part of the atmospheric correction methods~~, we do not apply an atmospheric correction to the measurements (radiances $L_{r,h}$) at flight altitude (h). ~~no such correction is applied to measured radiances at flight altitude h~~. Instead, we calculate and use the reflectance at flight altitude ~~in the snow-atmosphere system is calculated~~ by the following equation:

$$R = \frac{\pi L_{r,h}(\theta_i, \theta_r, \Delta\varphi)}{F_{0,\lambda}\cos\theta_i} \quad (4)$$

where $L_{r,h}$ is the measured radiance at flight altitude. All reflectance/BRF^e_λ values at flight altitude~~, presented~~ in this study represent ~~are calculated~~ R in~~using~~ Eq. 4 and are referred to as "reflectance factor" in the snow-atmosphere system.

In the simulation of the reflectance factor in a coupled snow-atmosphere system, ~~to~~ we need to account for atmospheric effects contribution properly~~,~~. ~~i~~For this reason, we take independent data about atmospheric parameters (Aerosol Optical Thickness (AOT) and gases absorption) from ground-based and space-borne measurements. We select the data with the closest~~at the~~ spatial and temporal interval ~~time and close to the location of~~ actual airborne measurements~~, are needed and taken from ground-based and space-borne measurements and applied to the simulation~~ We discuss m~~M~~ore details of the atmospheric data and their application to the simulation routine ~~are discussed~~ in sect. 3 and 4. To estimate BRF^e_λ just above the surface, further atmospheric correction is needed. We assume ~~at infrared wavelengths where atmospheric scattering is negligible,~~ the reflectance factor at flight altitude is a good estimation of BRF^e_λ just above the surface at infrared wavelengths where atmospheric scattering is negligible~~.~~.

3 Measurements

CAR is an airborne instrument, developed at NASA's Goddard Space Flight Center. It has been used during several field campaigns around the world since 1984 up to present. CAR has been used to measure the single scattering albedo of clouds~~, and~~ the bidirectional reflectance of various surface types and acquiring imagery of clouds and the Earth's surface~~, etc~~. For this study, we used CAR data from the ARCTAS campaign conducted at Elson Lagoon, near Barrow/Utqiaġvik, Alaska, in April 2008 as part of the International Polar Year (Lyapustin et al., 2010; Gatebe and King, 2016). The goal of ARCTAS was to study physical and chemical processes in the Arctic atmosphere and ~~surface~~(e.g. long-range transport of pollution to the Arctic) and surface parameters (e.g. snow reflectance angular variation)~~.~~ The P-3B aircraft carried CAR instrument and was deployed by NASA

from Fairbank. Fig. 1 shows the flight track on 7th of April 2008. The ~~D~~date, location, measurement geometry and available atmospheric parameters during the measurements used in this study are presented in Table 1.

The unique design of CAR provides simultaneously both up-welling and down-welling radiances at 14 spectral bands (Table 2) located in the atmospheric window regions of UV, visible and near-infrared from 0.34 µm to 2.3 µm comprising important wavelengths relevant for remote sensing applications such as aerosol retrievals. Through a rotating scan mirror, the instrument provides viewing geometries suitable for measurements needed for BRF calculation. CAR collects data by a mirror rotating 360° in a plane perpendicular to the direction of flight through a 190° aperture that allows acquiring data from local zenith to nadir or horizon to horizon with an angular resolution of 1°. The high angular/spatial resolution of 1° in both viewing zenith and azimuth angles allows the estimation of the anisotropy of the reflectance in the snow-atmosphere system with high accuracy.

~~allowed the anisotropy of the reflectance in the snow-atmosphere system to be estimated with high accuracy.~~

The spatial resolution of CAR depends on the flight altitude e.g. 10 m^2 and 18 m^2 at nadir for 600 m and 1000 m flight altitude, respectively, which increases with the viewing zenith angle (VZA) e.g. 580 m^2 at 80° VZA for 1000 m flight altitude. The capability of acquiring data at different altitudes (~ 200, 600 and 1700 m) enables us to evaluate the sensitivity of reflectance with respect to atmospheric effects in RTM simulations.

Examples of calculated reflectance factor values using Eq. (4) from CAR measurements on 7th of April, 2008 at Elson Lagoon (71.3° N, 156.4° W) are shown in Fig. 2 and Fig. 3. As we can see in these two figures, ~~I~~in spite of the influence of the atmospheric scattering and absorption, the general features of the snow BRF are clearly observable in polar plots as well as principal and cross plane plots: ~~The latter comprise:~~ i) the decrease of snow reflectance with increasing wavelength due to the increasing absorption by snow at longer wavelengths; ii) the increase of the snow BRF as a function of VZA and the strong forward scattering peak in the principal plane at large VZA; iii) the smaller angular variation of the BRF at cross plane compared to the principal plane~~.~~, though ~~T~~the reflectance values increase with VZA~~altitude~~. The snow surface spatial inhomogeneity decreases with increasing altitude due to the change of spatial resolution with altitude (Gatebe and King, 2016; Lyapustin et al., 2010). Accordingly, at poorer spatial resolution, spatial homogeneity are more efficiently averaged as can be seen in Fig. 2 at flight altitude of 1700 m compared to 206 m~~.~~ in which we have higher spatial resolution.

To account for aerosols, we use the Aerosol optical thickness~~,~~ (AOT) data acquired by the nearby Aerosol Robotic Network (AERONET) sun-photometer at Barrow/Utqiaġvik during the CAR measurement time. AERONET is a globally distributed network and provides long-term and continuous ground-based measurements of the total column aerosol optical thickness derived from the attenuation of sun light and

provided often at high temporal resolution of 15 minutes. AERONET AOT data are provided at 0.5 µm and 0.6 µm wavelengths. We use the Ångström exponent to calculate AOT values at the reference wavelength (0.55 µm) required for the SCIATRAN simulation. Table 1 shows the calculated AOT at 0.55 µm based on AERONET data for Barrow/Utqiaġvik at the closest time to the CAR airborne measurements. Aerosol condition and its chemical and optical properties have been measured ~~C~~continuously ~~measurements of chemical and optical properties of aerosol~~ at Barrow, Alaska, during different seasonal periods (Quinn et al., 2002). Previous studies indicate the largest contribution from sea salt, non-sea-salt sulfate and mineral dust. The average contribution of black carbon is very small compared to other aerosol types (Udisti et al., 2020). During the haze season (January to April), sea salt plays the dominant role in controlling light scattering in wintertime and non-sea salt sulfate in spring (Quinn et al., 2002). The increase on nss-sulfate in January to May is the long-range transport of anthropogenic primary nss sulfate besides the long-range transport of anthropogenic SO2 and its photo-oxidization to nss-sulfate with increase of light levels, and the local production of biogenic nss-sulfate.

To account for ozone absorption, we use knowledge of the ozone total column amount retrieved from the space borne measurements by using the University of Bremen weighting function DOAS (WFDOAS) algorithm version 4 (Weber et al., 2018). This~~e~~ data set~~dataset~~ (covering from 1995-present) consists of merged total ozone column data retrieved by WFDOAS from Global Ozone Monitoring Experiment (GOME), Scanning Imaging Absorption Spectrometer for Atmospheric Chartography (SCIAMACHY), and GOME-2A. In this paper, ~~T~~the ozone total column ~~WFDOAS~~ data are selected using the criteria of having smallest temporal and spatial differences with CAR data. For nitrogen dioxide, we use vertical column information from the SCIATRAN database obtained from a 2D chemical transport model developed at University of Bremen (Sinnhuber et al., 2009).

The derived AOT and trace vertical column have been used in the simulation of radiative transfer processes in the snow-atmosphere system.

4 Simulations

SCIATRAN is a software package for radiative transfer modeling, developed at the Institute of Environmental Physics (IUP), University of Bremen (Rozanov et al., 2002; 2014) and freely available at http://www.iup.uni-bremen.de/sciatran/. The SCIATRAN package has been used in a variety of remote sensing studies to simulate radiative transfer processes in the wide spectral range from the ultraviolet to the thermal infrared (0.18 µm - 40 µm), assuming either a plane parallel or a spherical atmosphere (Rozanov et al., 2014).

In this paper, ~~T~~to calculate reflectance factor values, SCIATRAN assumes that the snow is a layer with an optical thickness of 1000 and a geometrical thickness of 1 m composed of ice crystals of different morphologies and placed above a black surface. This assumption was successfully validated by Rozanov et al. (2014). The snow layer is assumed to be vertically and horizontally homogeneous and composed of a monodisperse population of ice crystals. The impact of impurities in the snow (e.g. black carbon) is neglected in this study. To simulate the radiative transfer through a snow layer, the single scattering properties of ice crystals including extinction and scattering efficiencies, single scattering albedo and phase functions need to be defined in SCIATRAN. All these parameters are dependent on the wavelength, size and shape of the particle (Leroux et al., 1999). Recently, a new data library of basic single scattering properties of nine ice crystal shapes/habits developed by Yang et al. (2013) has been incorporated in the SCIATRAN model (Pohl et al., ~~-~~2020 ~~Personal communication~~). This database comprises a full set of single scattering properties at wavelengths from the UV to the far IR for the following nine ~~eight~~ ice crystal morphologies: droxtal, column and hollow column, aggregate of eight columns, plates, small aggregate of five plates, large aggregate of ten plates, ~~and~~ hollow and solid bullet rosettes. More detailed information about the ice crystal shapes and sizes can be found in Yang et al. (2013). In addition to the above-mentioned nine~~eight~~ ice crystals, optical parameters for triadic Koch fractal (referred to as fractal in this paper) particles are used as well (Macke et al., 1996; Rozanov et al., 2014). The fractal particle model uses regular tetrahedrons as its basic elements. In this study, we use the second generation fractals as described in Macke et al. (1996) and Rozanov et al. (2014)~~. are utilized.~~

In SCIATRAN, the snow grains are specified by their single-scattering properties of sparsely distributed particles. Namely, the snow grains are assumed to be in the far field zones of each other and will thus scatter the light independently. For a snow layer, the snow grains can be located in each other's near-field, resulting in interactions between the scattered electromagnetic fields of neighboring particles which leads to modification of single-scattering properties (Mishchenko, 2014; Mishchenko, 1994). The impact of near-field effect was investigated in Pohl et al. (2019) using the modified single scattering properties of sparsely distributed particles as suggested in Mishchenko (1994). The comparison of snow BRFs calculated assuming sparsely or densely packed snow layers shows that the maximum difference does not exceed 0.015% (Pohl et al., 2019). Therefore, this effect was ignored in radiative transfer calculations through the snow layer.

To account for atmospheric effects, SCIATRAN incorporates a comprehensive database containing monthly and zonal vertical distribution of trace gases e.g. O_3, NO_2, SO_2, H_2O, etc., spectral characteristics of gaseous absorbers, vertical profiles of pressure and temperature and molecular scattering characteristics (see Rozanov et al., (2014) for details). To account for scattering and absorption by aerosols over snow in SCIATRAN, the

optical characteristics of aerosol particles and vertical distribution of aerosol number density are required. In this study we use Moderate Resolution Imaging Spectrometer (MODIS) collection 5 aerosol parameterization (Levy et al., 2007) as an internal database in SCIATRAN. Levy et al. (2007) developed a framework for connecting the aerosol micro-physical properties such as the refractive index and size distribution to the AOT at 0.55µm. Using AOT from ground-based measurements of AERONET at Barrow/Utqiaġvik as mentioned and selecting one of the aerosol types, the Mie code incorporated into SCIATRAN is employed to calculate aerosol extinction and scattering coefficients. In this study, the vertical profile of aerosol number density as an "exponential vertical distribution" for a height of 3.0 km is used.

For the conditions described above, the radiative transfer calculations are performed at a source-target-sensor geometry extracted from the airborne measurements at solar zenith angle of 70.23°, 69.11°, 67.68° and 62.11°; viewing zenith angle 0° - 70° and relative azimuth angle 0° - 360° with an angular resolution of 5° and at four different altitudes of 181 m, 206 m, 647 m and 1700 m. More detailed information about atmospheric and snow layer parameters are given and discussed separately in the following section.

5 Sensitivity of reflectance to the snow morphology and atmospheric parameters

The measured reflectance in the visible and NIR spectral range over a snow field depends on the relative importance of the absorption and scattering radiative transfer processes in the atmosphere and snow layer. In this section, we investigate the sensitivity of the reflectance on the radiative transfer through the atmosphere and the snow at the selected wavelength bands: i) 1.649 µm because of the high sensitivity of this wavelength to snow grain properties; and ii) 0.677 and 0.873 µm wavelengths because of the relatively high and differing sensitivities at these wavelengths to the atmospheric conditions and being used for aerosol optical thickness retrievals.

5.1 Impact of snow: size and shape of ice crystals

To study the influence of ice crystal morphology on the radiation field above ~~snow-covered~~snow-covered surfaces, we perform the simulation at 1.649 µm for three important reasons (Leroux et al., 1998):

i) the absorption of ice crystals is small or negligible at the selected wavelengths in the visible domain of the spectrum. In contrast, in the near-infrared range, due to the large absorption of ice crystals at these wavelengths, the snow reflectance is significantly affected by the snow grain size; the larger the particle, the smaller the reflectance because of larger absorption and stronger forward scattering;

ii) the BRF properties of snow at 1.649 µm are closer to that for single scattering behavior and it is linked to the phase function, ~~matrix~~ which strongly depends on the shape of ice crystals;

iii) the impact of the atmosphere (absorption by CO_2 and H_2O and diffuse incident irradiance) at 1.649 µm is negligible.

To illustrate the high sensitivity of radiation field to the varying size of ice crystals at 1.649 µm, we simulated snow reflectance factor at principal and cross planes assuming nine ice crystal morphologies with varying sizes (here size refers to maximum dimension/edge length) 60 ~ 10000 µm and three different roughness (smooth surface: 0, moderate surface roughness: 0.03, severe surface roughness 0.5), for further information see Yang et al. (2013). Fig. 4 shows the simulated reflectance factor versus the VZA in the principal plane (as the most sensitive and representative direction for the largest changes of reflectance) using severely roughened morphology. As can be seen in Fig. 4, the reflectance factor strongly changes with the size of ice crystals from 60 to 10000 µm. The equivalent effective radius[1] is shown besides the maximum lengths of ice crystals in Fig. 4. Differentiating between various shapes has the largest effect in forward scattering (φ=0°) and lesser effect in backward scattering direction (φ=180°). The results indicate that the effect of changing size is larger than the impact of differentiating between various shapes of ice crystals at this wavelength.

Using the "aggregate of 8 columns" shape and changing maximum dimension from 60 µm to 10000 µm result in reflectance decrease of ~ 40 % at nadir (VZA ~ 0°) and more than 80 % in forward scattering direction (at VZA of 60°) which is considerably large. If we change only the shape of snow grain from "aggregate of 8 columns" to the "droxtal", but we keep the size (largest dimension) as it is (e.g. 300 µm) ~~Changing the shape to the droxtal at the same size,~~this change provides a noticeable decrease of ~ 30% in reflectance at forward scattering direction for a viewing zenith angle of 60° and leads to a much weaker forward peak. Noteworthy is, that the plate shape cannot reproduce the enhancement in backward direction (typical for a BRF over snow) as strong as the "aggregate of 8 columns" or the "droxtal" shape cause. Using the "aggregate of 5 and 10 plates" leads to larger reflectance in all directions compared to the single "plate" shape. However, the analysis of simulation results at cross plane (not shown here) indicates that, the impact on the reflectance pattern, originating from the specific shapes of the ice crystals is relatively small compared to the impacts at principal plane.

The large range of changes of the reflectance in both the principal and cross planes, when using different ice crystal morphologies~~sizes in both the principal and cross planes~~ highlights the importance of having accurate a

1 Effective radius= 3/4 ×(V_{tot}/A_{tot}); V_{tot}: total volume and A_{tot}: the total projected area of ice per unit volume of air (Baum et al., 2014).

priori knowledge or estimation of size and shapes of the ice crystals ~~and their shapes~~ to accurately reproduce ~~simulate accurately~~ measurements. In our study, due to the lack of such information from in situ measurements, we estimate the size of ice crystals for each selected crystal shape separately to have a priori knowledge of ice crystal properties and limit the differences between the simulated and measured reflectance. The detailed explanation and results are given in sect. 6.

5.2 Impact of atmosphere: scattering and absorption by aerosol and gases

The incident radiation ~~on the snow layer~~ is composed of direct sunlight and the diffuse radiation from the sky (Aoki et al., 1999). To take the atmospheric absorption and scattering into account, we assume an atmosphere over the snow layer, which contains: i) Rayleigh scattering (scattering by air molecules), ii) gaseous absorption and iii) absorption and scattering by aerosols. Therefore, in this section, absorption bands e.g. 0.677 µm are selected to evaluate the impact of the atmosphere. We calculate the reflectance factor at 0.677 µm under three different conditions, assuming a model atmosphere governed: i) by Rayleigh scattering; ii) identical to i) but with absorption by ozone (O_3) and nitrogen dioxide (NO_2); iii) identical to ii) but including aerosol. The calculations are performed assuming the following properties of the atmosphere and snow layer:

i) Vertical profile of nitrogen dioxide, pressure and temperature are selected according to a 2D chemical transport model (Sinnhuber et al., 2009) incorporated in SCIATRAN;

ii) Total vertical column of ozone as well as AOT are set according to Table 1;

iii) Snow layer is composed of ice crystals having the shape "aggregate of 8 column", maximum dimension of 650 µm and severely roughened crystal surface.

Fig. 5 shows the impact of the atmosphere and the difference between measured and simulated reflectance factor values at three different altitudes: 206, 647 and 1700 m; for the 3 scenarios. The reflectance reduction at 647 m flight altitude due to gaseous absorption is the smallest ~ 5% close to the nadir region and becomes larger ~ 10% in forward scattering direction which decreases to ~ 8% at 1700 m altitude. At this wavelength, ozone with vertical optical depth (VOD) of 1.6×10^{-2} has a much larger contribution to gaseous absorption as compared to that of NO_2 with VOD of 3.95×10^{-5}.

The reflectance for an atmosphere containing three types of aerosol (weakly/moderately/strongly absorbing aerosol) and without aerosol (containing only Rayleigh and gaseous absorption) are presented in Fig. 5. For more information on aerosol typing used in this study ~~please~~ see Levy et al. (2007). The changes in reflectance due to weakly absorbing aerosol with an AOT of 0.11 (measured by AERONET) at 206 m flight altitude are ~ 5% at nadir and increase in forward scattering direction to ~ 13%. The strongly absorbing aerosol (at the same

AOT of 0.11) reduces the reflectance by ~7% at nadir and ~ 20 % in forward scattering direction. At 1700 m, the reflectance decreases by 6% at nadir and 7% in forward scattering direction. The differences between the three aerosol types does not lead to changes in reflectance, which are larger than 5% in or close to nadir areas. In summary, an atmosphere containing Rayleigh scattering, absorption by ozone (O_3) and nitrogen dioxide (NO_2) and weakly absorbing aerosol is the best representation of the atmospheric conditions for our case study.

6 Retrieval of snow grain size and shape

In the previous section, we showed that having adequate a priori information about snow surface and atmosphere is necessary to calculate reflectance factor of sufficient accuracy. In contrast to the atmospheric parameters available from independent sensors and models, a priori knowledge about ice crystal size and shape for the underlying snow layer is not typically available. To estimate the optimal ice crystal morphology we used a snow grain size and shape retrieval algorithm, by minimizing the difference between the measured and simulated reflectance factor (See appendix A for details). Here size refers to effective radius[2] of the ice crystal. The retrieval algorithm is applied to measurements at principal and cross planes at 1.649 µm assuming different shape and crystal surface roughnesses. To find the best representative shape and size, the bias and Root Mean Square Error (RMSE) between the measured and simulated reflectance factor were determined for each case study.

Fig. 6 shows one example of the comparison between measured and simulated reflectance factor at principal and cross planes. The absolute uncertainty of CAR measurements is within 5% and shown by uncertainty envelope. The accuracy of our radiative transfer calculations is estimated to be in the range of 0.1 %. Based on comparison, one can state that the angular reflectance pattern of the CAR measurement on the 7th of April 2008 at Elson Lagoon is reproduced by SCIATRAN successfully. The highest accuracy is obtained by assuming ice crystals as "an aggregate of 8 columns" with severely roughened crystal surface at an effective radius of 98.8 µm (corresponding to maximum dimension of 650 µm). In this case, the largest and smallest discrepancies appear in the forward scattering direction and close to nadir (VZA< ± 25°), respectively. The overall RMSE and bias between measurements and simulation at principal plane is 6.9 % and 2.7 % respectively. A lesser degree of agreement between simulated results and measurements are provided by using "column" and fractal shapes with an RMSE of 7.3% and 9.75%, respectively. The largest difference between measurements and simulations is observed for the case using "droxtal" shape with an RMSE ~ 25.54%.

2 ~~effective radius= 3/4 ×(V_{tot}/A_{tot}); V_{tot}: total volume and A_{tot}: the total projected area of ice per unit volume of air (Baum et al., 2014).~~

We also retrieved effective radius of ice crystal using CAR data for fresh fallen snow on the 15th of April 2008. Due to the existing surface horizontal inhomogeneity for the case of fresh snow acquired at lower flight altitude ~ 181 m, larger differences between simulated and measured reflectance are expected, as compared to the old snow case on the 7th of April 2008. The results are shown in Fig. 7. Unlike the old snow case presented in Fig. 6, the "aggregate of 8 columns" shape does not optimally represent the ice crystals of this particular day. Rather, a reflectance simulated by using an "aggregate of 5 plates" as the ice crystal shape provides the minimum RMSE ~ 12.85% between measurement and simulation results. "Aggregate of 10 plates" and fractal provide the second and third most representative shapes with an RMSE of ~ 13.16 % and 14.69 %, respectively. The results obtained by using the "droxtal" ice crystal shape exhibit large differences in both of forward and backward scattering directions with RMSE of 34.1 %.

Though the real nature of ice crystal shape at the time of measurement is not known to us, the impact of temperature and supersaturation on morphology of snow grain particles has been debated in previous studies. ~~The results of such studies are now compared with our findings~~ (Slater and Michaelides, 2019; Shultz, 2018; Libbrecht, 2007; Bailey and Hallett, 2004; Yang et al., 2003). Based on the relationship between temperature and snow grain morphology, the column-based shapes are the dominant ice crystal morphology in environments with temperatures higher than -10°C whereas plates are dominant if the temperature is less than -10°C. Though, more investigation is needed especially to account for the temperature profile at the exact time of snowfall, ~~O~~our findings with respect to the most representative shape for each case study agree with this argument. The temperature range during CAR measurements at 6-7th of April 2008 is from -20 to -5°C. Based on our results the "aggregate of 8 columns" is the most representative shape for measurements conducted on this day. On 15th of April 2008 when the temperature range changes to -23 to -17°C, mainly plate-based ice crystal shapes are expected for such low temperatures and our results confirm this argument. In addition, the existence of droxtal ice crystals during the measurement is less probable because very low temperatures (~ -50°C) are needed to form droxtal or quasi-spherical ice crystals (Yang et al., 2003). The temperature dependence of the ice crystal morphologies explains in part why droxtal shaped ice crystals do not capture the derived snow reflectance values from CAR measurements in any of our scenarios. With respect to size of ice crystals, we do not compare fresh and old snow cases because it is important to note that the date of old snow case is before fresh snow. This means the studied old snow case is not the aged fresh snow case. Therefore, the change of ice crystal size with its age is not studied in the scope of this paper.

A summary of retrieved effective radii using different ice crystal shapes and corresponding bias and RMSE values is presented in Table 3~~2~~. The ice crystals with minimum RMSE value at 1.649 µm are underlined and

selected to be used for subsequent calculations of reflectance factor at 0.677, 0.873 µm. In Fig. 8, the importance of ice crystal shape selection for the snow grain size retrieval and the snow reflectance calculation is highlighted. The measurements were selected from the old snow and fresh snow cases. The effective radius is retrieved only at 1.649 µm and then has been used to calculate the reflectance factor at 0.677 µm and 0.873 µm. The results are presented in Fig. 8 with corresponding RMSE and bias values in the principal plane. The uncertainty of effective radius retrieval is estimated to be ~10% on the base of optimal estimation technique and is shown by gray envelope in Fig. 8. It can be seen that the retrieved effective radius value changes from shape to shape. The difference in retrieved effective radius generally does not exceeds 40 % but in the case of the plate ice crystals the retrieved effective radius is ~70 % smaller than the other shapes e.g. aggregate of 8 columns. This is a significantly large difference. However, these results are presented for the principal plane where the maximum differences between simulation and measurement is expected. Therefore, the overall bias and RMSE value on all azimuth direction is smaller than presented here. It can be seen that the RMSE values at 0.677 µm and 0.873 µm are significantly smaller than that at 1.649 µm. This is explained by the high reflectance values at these wavelengths and therefore the larger denominator in RMSE formula, in which the difference of measured and simulated reflectance factor is divided by measured reflectance.

7 Comparison of measured and simulated reflectance factor

In this section we present results of the comparison of measured and simulated reflectance factor in the snow-atmosphere system. The simulations, which used the results and findings described in ~~the based on~~ the previous section were performed: assuming an atmosphere containing O_3, NO_2, weakly absorbing aerosol as described in Table 1. The snow layer is assumed to be comprised of "aggregate of 8 column" ice crystals with a maximum dimension of 650 µm (effective radius ~~98.83~~99 µm) for the case of old snow, and "aggregate of 5 plates" ice crystals with a maximum dimension of 725 µm (effective radius 83~~83.41~~ µm) for the case of fresh snow. ~~To assess the accuracy of simulations over all azimuth angles, the correlation plot and the Pearson correlation coefficient between measured and modeled reflectance are shown in Fig. 11.~~

In Fig. 9, the difference between the simulated and measured reflectance factor at 0.677 and 1.649 µm is small on average, being less than 0.025 in regions of small VZA and not exceeding ±0.05 for larger VZA < 50°. These values are larger at 0.873 µm; the maximum difference reaches ~ ±0.05 for small VZA. The difference between SCIATRAN simulation values and those of the measurements is pronounced in the forward scattering region where $|\Delta\varphi| < 40°$. ~~As it is shown in Fig. 11, the correlation coefficient between reflectance measurements over old snow and simulation is high, ~ 0.98.~~ Fig. 10 is the same plot as Fig. 9 but for fresh snow. The

differences between SCIATRAN simulations and CAR measurements of the reflectance factor are less pronounced in the glint region, as compared to those for the old snow.

To assess the accuracy of simulations over all azimuth angles, the correlation plot and the Pearson correlation coefficient between measured and modelled reflectance factor are shown in Fig. 11. As it is shown in Fig. 11, the correlation coefficient between reflectance measurements over old snow and simulation is high, ~ 0.98. We consider that surface inhomogentities and related larger shadowing effects at measurement altitude of 181 m, explain why the correlation decreased to 0.88 at 0.677 μm (for the case of old snow, acquired at 647 m flight altitude, surface inhomogenities are smoothed and therefore the old snow case is less affected by surface inhomogenities). However, in Fig. 11, at 1.649 μm correlation coefficient is high ~ 0.97 for the case of fresh snow, possibly because of their being less sensitivity of this channel to shadowing and atmospheric scattering effects. ~~In addition, the high correlation coefficient at 1.649 μm and small discrepancies < ±0.025 in off-glint region confirms the suitability of the selection of the best representation for ice crystal shape in previous step. The differences between SCIATRAN simulations and CAR measurements of reflectance are less pronounced in the glint region, as compared to those for the old snow.~~

8 Conclusion

In this study, our objective was to assess the accuracy of the simulation of the reflectance in a snow-atmosphere system taking different snow morphology and atmospheric absorption and scattering into account. For this we used a state of the art RTM, SCIATRAN, which used explicit models of the snow layer and the airborne CAR measurements.

The airborne CAR data were acquired by NASA over Elson Lagoon at Barrow/Utqiaġvik, Alaska, during the ARCTAS campaign in spring 2008. The spectral coverage of the airborne measurements is wide (0.3-2.30 μm) comprising important wavelengths relevant for remote sensing applications such as aerosol retrievals which could benefit from the results of this study. Measurements obtained at different flight altitudes (~ 200, 600 and 1700 m) provide an opportunity to investigate the sensitivity of simulated reflectance to atmospheric parameters.

The SCIATRAN RTM (a phenomenological RTM) was used to simulate the reflectance factor in the snow-atmosphere system and its changes for different snow morphologies (i.e. snow grain size and shape). These simulations take atmospheric scattering and absorption explicitly into account. We investigated the sensitivity of reflectance in the snow-atmosphere system to snow grain size and shape. We have shown that the selection of the most representative shape and size of the nine ice crystals used in SCIATRAN to describe the snow surface is essential to minimize the difference between simulations and measurements.

To obtain a priori knowledge of snow morphology, we use the snow grain size and shape retrieval algorithm and apply it to CAR data. In our case study at Barrow/Utqiaġvik, the simulated reflectance factor assuming ice crystals with aggregate composed of 8 columns shape agreed well with measurements for the old snow case, having RMSE of 6.9 % and average bias of 2.7 % with respect to the measured CAR reflectance in the principal plane where the largest discrepancies are expected. For the case of freshly fallen snow, an aggregate of 5 plates shape was the most representative ice crystal having RMSE values of 12.8 % and a bias of 11.23 % with respect to the measured CAR reflectance. The data for the freshly fallen snow case were acquired at 181 m. Larger differences as compared to the older snow case at 647 m are attributed to surface inhomogenity. The surface inhomogenity most likely originate from sastrugi. Simulation, in which the snow layer was comprised of ice crystals with a droxtal shape (being semi-spherical particles) did not yield accurate reflectance for the snow-atmosphere system in any of our case studies. We showed that using the knowledge from studies of the temperature dependence of ice crystal morphologies agrees with our findings with respect to the most representative ice crystal size and shape for our case studies.

In our study, the simulated patterns of the reflectance factor with respect to spectral and directional signatures produce well the measurements, as evidenced by the high correlation coefficients in the range of 0.88 ~ 0.98 between measurements (old and fresh snow) and simulation at the selected wavelengths of 0.677, 0.873 and 1.649 μm. In the off-glint regions $|\Delta\varphi| > 40°$ and VZA < 50°, the overall absolute difference between the modeled reflectance factor from SCIATRAN and CAR measurements is below 0.05. This absolute difference in off-glint area is smaller in the short wave infrared as compared to visible. It should be noted here that the reflectance of the snow is lower in the short wave infrared compared to the visible.

In summary, the approach shows the high accuracy of the phenomenological SCIATRAN RTM in simulating the radiation field in the snow-atmosphere scenes for off-glint observations. The results are applicable for the inversion of snow and atmospheric data products from the satellite or airborne passive remote sensing measurements above snow. To mitigate the relatively larger differences between measurements and simulation for glint condition as compared to off-glint region, the use of a vertically inhomogeneous snow layer consisting of different ice crystal shapes and sizes is proposed.

This research has been undertaken as part of the investigations in the framework of trans regional (AC)3 project (Wendisch et al., 2017) that aims to identify and quantify different parameters involved in rapidly changing climate in the Arctic. In this respect, the analysis of this study will be used to improve the assumptions made for reflectance in snow-atmosphere system in the algorithms designed to retrieve atmospheric parameters (such as AOT) above Polar Regions.

Appendix

For the selected snow models using different ice crystal morphologies, the variation of the snow reflectance $R(\lambda,\Omega)$ at wavelength λ and direction Ω with respect to the variation $\delta r_e(z)$ of the effective radius profile $r_e(z)$ along the vertical coordinate z within snow layer can be presented, neglecting nonlinear terms, by the following equation:

$$R(\lambda,\Omega)=R_0(\lambda,\Omega)+\int_0^{Zt} W_r(z,\lambda,\Omega)\delta r_e(z)dz, \quad (1)$$

where $R_0(\lambda,\Omega)$ and $R(\lambda,\Omega)$ are the reflection functions calculated assuming an effective radius profile $\acute{r}_e(z)$ and $\acute{r}_e(z)+\delta r_e(z)$, respectively. The angular variable $\Omega=\{\theta_0,\theta,\varphi\}$ comprises a set of variables: θ_0 is the solar zenith angle, θ and φ are the zenith and relative azimuthal angles of observation direction; Z_t is the top altitude of snow layer and

$$W_r(Z,\lambda,\Omega)=\frac{\delta R(\lambda,\Omega)}{\delta r_e(z)}, \quad (2)$$

is the functional derivative of the function $R(\lambda,\Omega)$ with respect to the function $r_e(z)$ which is also called weighting function (Rozanov et al., 2007). The weighting function was calculated using a numerically efficient forward-adjoint approach (Rozanov, 2006; Rozanov and Rozanov, 2007) implemented in the SCIATRAN model. Here, it is assumed that properties of snow do not change in the horizontal plane and within snow layer there is no additional absorber such as soot, dust or other pollutants. We note that the weighting function includes the contribution of variations not only by the scattering and extinction coefficients but also by the phase function.

Although the linear relationship given by Eq. (1) can be used to retrieve the vertical profile of the effective radius within the snow layer in a way similar to that used to the morphology of water droplets (Kokhanovsky and Rozanov, 2012), we restrict ourselves to the assumption of independent of the altitude r_e. Introducing the weighting function for the absolute variation of the effective radius as:

$$W_r(\lambda,\Omega)=\int_0^{Zt} W_r(z,\lambda,\Omega)dz, \quad (3)$$

we have

$$R(\lambda,\Omega)=R_0(\lambda,\Omega)+W_r(z,\lambda,\Omega)\delta r_e. \quad (4)$$

The resultant linear relationship is a basic equation to formulate inverse problem with respect to the parameter r_e using measurements of spectral reflectance.

For practical applications Eq. (4) should be rewritten in the vector-matrix form as follows:

$$Y - Y_0 = K\left(X - X_0\right). \quad (5)$$

The components of vectors Y and Y_0 are the measured and simulated reflectance at discrete number of observation directions Ω_j and wavelengths λ_i, the elements of matrix K are weighting functions $W_r\left(\lambda_i, \Omega_j\right)$, X=[r_e] is the state vector, $X_0 = \left[\acute{r}_e\right]$ is the a priori state vector. We note that in the case under consideration, the matrix K and state vector X are represented by the column vector and scalar, respectively.

Assuming that the number of discrete observation directions Ω_j and wavelengths λ_i is larger than the dimensions of the state vector, the solution of Eq. (5) is obtained by minimizing the following cost function:

$$\Delta = \left\| Y - Y_0 - K\left(X - X_0\right) \right\|^2, \quad (6)$$

which describes the root-mean-square deviation between measured and simulated snow reflectance.

Owing to the linear relationship given by Eq. (5) the minimization problem formulated above can be solved analytically:

$$X = X_0 + \left(K^T K\right)^{-1} K^T \left(Y - Y_0\right). \quad (7)$$

In deriving Eq. (7) we have neglected the linearization error which can be significant if X_0 is far from X. To mitigate the impact of linearization error we solve minimization problem given by Eq. (6) iteratively. In particular instead of Eq. (7) is used

$$X_n = X_{n-1} + \left(K_{n-1}^T K_{n-1}\right)^{-1} K_{n-1}^T \left(Y - Y_{n-1}\right), \quad (8)$$

Where n=1, 2, … is the iteration number, K_{n-1} and Y_{n-1} are the matrix of weighting functions and reflectance vector calculated using the state vector X_{n-1}. The iteration process is finished if the difference between X_n and X_{n-1} is smaller than a preselected criteria.

The calculation of weighting functions and ~~TOA~~ reflectance at flight altitude is performed at each iteration step using the radiative transfer model SCIATRAN (Rozanov et al., 2014). In SCIATRAN weighting functions are calculated employing a very efficient forward-adjoint technique, which is based on the joint solution of the linearized forward and adjoint radiative transfer equations (Rozanov 2006; Rozanov and Rozanov 2007 and references therein). This enables the TOA reflectance and required weighting function to be calculated simultaneously.

Acknowledgement

We gratefully acknowledge the funding by the Deutsche Forschungsgemeinschaft (DFG, German Research Foundation) – Project Number 268020496 – TRR 172, for SJ within the Transregional Collaborative Research Center "ArctiC Amplification: Climate Relevant Atmospheric and SurfaCe Processes, and Feedback Mechanisms (AC)3". We thank Christine Pohl for her contribution to the extension of ice crystal property database in SCIATRAN.

References

Aoki, Te., Aoki, Ta., Fukabori, M., and Uchiyama, A.: Numerical simulation of the atmospheric effects on snow albedo with a multiple scattering radiative transfer model for the atmosphere-snow system, J. Meteorol. Soc. Jpn., 77, 595–614, https://doi.org/10.2151/jmsj1965.77.2_595, 1999.

Arnold, G. T., Tsay, S.-C., King, M. D., Li, J. Y., Soulen, P. F.: Airborne spectral measurements of surface-atmosphere anisotropy for arctic sea ice and tundra, Int. J. Remote Sens., 23(18), 3763–3781, https:/doi.org/10.1080/01431160110117373, 2002.

Arrhenius, S.: On the influence of carbonic acid in the air upon the temperature of the ground. Mag. J. Sci., London, Edinburgh, Dublin Phil, 41, 237-276, 1896.

Bailey, M. and Hallett, J.: Growth rates and habits of ice crystals between -20C and -70C, J. Atmos. Sci., 61, 514–544, https://doi.org/10.1175/1520-0469(2004)061<0514:GRAHOI>2.0.CO;2, 2004.

Barkstrom, B.: Some Effects of Multiple Scattering on the Distribution of Solar Radiation in Snow and Ice, J. Glaciol., 11(63), 357-368, https://doi.org/10.3189/S0022143000022334, 1972.

Baum, B., Yang, P., J. Heymsfield, A., Bansemer, A., H. Cole, B., Merrelli, A., Schmitt, C., Wang, C.: Ice cloud single-scattering property models with the full phase matrix at wavelengths from 0.2 to 100 μm, J. Quant. Spectrosc. Ra., 146, 123-139, https://doi.org/10.1016/j.jqsrt.2014.02.029, 2014.

Cohen, J., Screen, J. A., Furtado, J., C., Barlow, M., Whittleston, D., Coumou, D., Francis, J., Dethloff, K., Entekhabi, D., Overland, J., Jones, J.: Recent Arctic amplification and extreme mid-latitude weather, Nat. Geosci., 7, 627–637, https://doi.org/10.1038/ngeo2234, 2014.

Curry, J. A., Schramm, J. L., Ebert, E. E.: Sea Ice-Albedo Climate Feedback Mechanism, J. Climate, 8, 240–247, https://doi.org/10.1175/1520-0442(1995)008<0240:SIACFM>2.0.CO;2, 1995.

Dunkle, R.V. and Bevans, J.T.: An approximate analysis of the solar reflectnce and transmittance of a snow cover, J. Meteorol., 13, 212–216, https://doi.org/10.1175/15200469(1956)013<0212:AAAOTS>2.0.CO;2, 1956.

Gatebe, C. K., King, M. D., Lyapustin, A. I., Arnold, G. T., Redemann, J.: Airborne spectral measurements of ocean directional reflectance, J. Atmos. Sci., 62, 1072–1092, https://doi.org/10.1175/JAS3386.1, 2005.

Gatebe, C. & King, M.: Airborne spectral BRDF of various surface types (ocean, vegetation, snow, desert, wetlands, cloud decks, smoke layers) for remote sensing applications, Remote Sens. Environ., 179, 131-148. 10.1016/j.rse.2016.03.029, 2016.

Hudson, S. R., Warren, S. G., Brandt, R. E., Grenfell, T. C., Six, D.: Spectral bidirectional reflectance of Antarctic snow: measurements and parameterization, J. Geophys. Res., 111, D18106, https://doi.org/10.1029/2006JD007290, 2006.

Hudson, S. R. and Warren, S. G.: An explanation for the effect of clouds over snow on the top-of atmosphere bidirectional reflectance, J. Geophys. Res., 112, D19202, https://doi.org/10.1029/2007JD008541, 2007.

Istomina, L. G., von Hoyningen-Huene, W., Kokhanovsky, A. A., and Burrows, J. P.: The detection of cloud-free snow-covered areas using AATSR measurements, Atmos. Meas. Tech., 3, 1005–1017, https://doi.org/10.5194/amt-3-1005-2010, 2010.

Istomina, L.: Retrieval of aerosol optical thickness over snow and ice surfaces in the Arctic using Advanced Along Track Scanning Radiometer, PhD thesis, University of Bremen, Bremen, Germany, 2012.

Jafariserajehlou, S., Mei, L., Vountas, M., Rozanov, V., Burrows, J. P. and Hollmann, R.: A cloud identification algorithm over the Arctic for use with AATSR-SLSTR measurements, Atmos. Meas. Tech., 12, 1059-1076, https://doi.org/10.5194/amt-12-1059-2019, 2019.

Jin, Z., Charlock, T. P., Yang, P., Xie, Y., Miller, W.: Snow optical properties for different particle shapes with application to snow grain size retrieval and MODIS/CERES radiance comparison over Antarctica, Remote Sens. Environ., 112, 3563–3581, https://doi.org/10.1016/j.rse.2008.04.011, 2008.

Kim, B. M., Hong, J. Y., Jun, S. Y., Zhang, X., Kwon, H., Kim, S. J., Kim, J. H., Kim, S. W., Kim, H. K.: Major cause of unprecedented Arctic warming in January 2016: critical role of an Atlantic windstorm, Sci. Rep-UK, 7, 40051, https://doi.org/10.1038/srep40051, 2017.

Kokhanovsky, A. A., and Zege, E. P.: Scattering optics of snow, Appl. Optics., 43, 1589–1602. https://doi.org/10.1364/AO.43.001589, 2004.

Kokhanovsky, A. A., Aoki, T., Hachikubo, A., Hori, M., and Zege, E. P.: Reflective properties of natural snow: approximate asymptotic theory versus in situ measurements, IEEE Transactions on Geoscience and RemoteSensing, 43, 1529-1535, doi: 10.1109/TGRS.2005.848414, 2005.

Kokhanovsky, A. A., Budak, V. P., Cornet, C., Duan, M., Emde, C., Katsev, I. L., Klyukov, D. A., Korkin, S. V., C-Labonnote, L., Mayer, B., Min, Q., Nakajima, T., Ota, Y., Prikhach, A. S., Rozanov, V. V., Yokota, T., Zege, E. P.: Benchmark results in vector atmospheric radiative transfer, J. Quant. Spectrosc. Ra., 111, 1931–46, https://doi.org/10.1016/j.jqsrt.2010.03.005, 2010.

Kokhanovsky, A., Rozanov, V.V., Aoki, T., Odermatt, D., Brockmann, C., Krüger, O., Bouvet, M., Drusch, M., Hori, M.: Sizing snow grains using backscattered solar light, Int. J. Remote Sens., 32:22, 6975-7008, https://doi.org/10.1080/01431161.2011.560621, 2011.

Kokhanovsky, A. A., and Breon, F.: Validation of an Analytical Snow BRDF Model Using PARASOL Multi-Angular and Multispectral Observations, IEEE Geosci. Remote S., 9, 928-932, 10.1109/LGRS.2012.2185775, 2012.

Kokhanovsky, A. A. and Rozanov, V. V.: Droplet vertical sizing in warm clouds using passive optical measurements from a satellite, Atmos. Meas. Tech., 5, 517-528, https://doi.org/10.5194/amt-5-517-2012, 2012.

Leroux, C., Deuzé, J.-L., Goloub, P., Sergent, C., Fily, M.: Ground measurements of the polarized bidirectional reflectance of snow in the near-infrared spectral domain: Comparisons with model results, J. Geophys. Res., 103(D16), 19721–19731, https://doi.org/10.1029/98JD01146, 1998.

Leroux, C., Lenoble, J., Brogniez, G., Hovenier, J.W., De Haan, J.F.: A model for the bidirectional polarized reflectance of snow, J. Quant. Spectrosc. Ra., 61, 3, 273-285, https://doi.org/10.1016/S0022-4073(97)00221-5, 1999.

Levy, R.C., Remer, L.A., Mattoo, S., Vermte, E. F., Kaufman, Y.J.: Second-generation operational algorithm: Retrieval of aerosol properties over land from inversion of Moderate Resolution Imaging Spectroradiometer spectral reflectance, J. Geophys. Res., 112, D13211, https://doi.org/10.1029/2006JD007811, 2007.

Li, S., and Zhou, X., Modelling and measuring the spectral bidirectional reflectance factor of snow-covered sea ice: An intercomparison study. Hydrol. Process. 18(18), 3559–3581, https://doi.org/10.1002/hyp.5805, 2004.

Libbrecht, K. G.: The formation of snow crystal, Am. Sci., 95, 52–59, 2007.

Lyapustin, A., Gatebe, C. K., Kahn, R., Brandt, R., Redemann, J., Russell, P., King, M. D., Pedersen, C. A., Gerland, S., Poudyal, R., Marshak, A., Wang, Y., Schaaf, C., Hall, D., Kokhanovsky, A. A.: Analysis of

snow bidirectional reflectance from ARCTAS spring-2008 campaign, Atmos. Chem. Phys., 10, 4359–75, https://doi.org/10.5194/acp-10-4359-2010, 2010.

Macke, A., Mueller, J., Raschke, E.: Scattering properties of atmospheric ice crystals, J. Atmos. Sci., 53, 2813–25, https://doi.org/10.1175/1520-0469(1996)053<2813:SSPOAI>2.0.CO;2, 1996.

Middleton, W., & Mungal, A.: The luminous directional reflectance of snow, J. Opt. Soc. Am., 42(8), https://doi.org/10.1364/JOSA.42.000572, 1952.

Mishchenko, M. I.: Asymmetry parameters of the phase function for densely packed scattering grains, J. Quant. Spectrosc. Ra., 52, 95–110, https://doi.org/10.1016/0022-4073(94)90142-2, 1994.

Mishchenko, M. I., Dlugach, J. M., Yanovitskij, E. G., Zakharova, N. T.: Bidirectional reflectance of flat, optically thick particulate layers: an efficient radiative transfer solution and applications to snow and soil surfaces, J. Quant. Spectrosc. Ra., 63, 409–432, https://doi.org/10.1016/S0022-4073(99)00028-X, 1999.

Mishchenko, M. I.: Directional radiometry and radiative transfer: The convoluted path from centuries-old phenomenology to physical optics, J. Quant. Spectrosc. Ra., 146, 4–33, https://doi.org/10.1016/j.jqsrt.2014.02.033, 2014.

Negi, H. S. and Kokhanovsky, A.: Retrieval of snow albedo and grain size using reflectance measurements in Himalayan basin, The Cryosphere, 5, 203-2017, 10.5194/tc-5-203-2011, 2011.

Nicodemus, F. E.: Directional reflectance and emissivity of an opaque surface, Appl. Optics., 4, 767−773, https://doi.org/10.1364/AO.4.000767, 1965.

Nicodemus, F. E., Richmond, J. C., Hsia, J. J., Ginsberg, I. W., Limperis, T.: Geometrical considerations and nomenclature for reflectance, in: Wolff, L. B., Shafer, S. A., and Healey, G. (Eds.), Radiometry. Jones and Bartlett Publishers, Inc., USA, pp. 94-145, http://dl.acm.org/citation.cfm?id=136913.136929, 1977.

Painter, T. H., Dozier, J., Roberts, D. A., Davis, R. E., Greene, R. O.: Retrieval of subpixel snow-covered area and grain size from imaging spectrometer data, Remote Sens. Environ., 85, 64–77, https://doi.org/10.1016/S0034-4257(02)00187-6, 2003.

Pohl, C., Rozanov, V., Wendisch, M., Spreen, G., Heygster, G.: Impact of near-field effect on bidirectional reflectance factor and albedo of snow calculated by a phenomenological radiative transfer model, J. Quant. Spectrosc. Ra., https://doi.org/10.1016/j.jqsrt.2019.106704, 2020.

Pohl, C., Rozanov, V. V., Mei, L., Burrows, J. P., Heygster, G., Spreen, G., ~~et al.~~: Implementation of an extensive ice crystal single-scattering property database in the radiative transfer model SCIATRAN, J. Quant. Spectrosc. Ra., 253, https://doi.org/10.1016/j.jqsrt.2020.107118, 2020. ~~Personal communication~~.

Quinn, P. K., Miller, T. L., Bates, T. S., Ogren, J. A., Andrews, E., & Shaw, G. E.: A 3-year record of simultaneously measured aerosol chemical and optical properties at Barrow, Alaska., J. Geophys. Res., Atmos., 107(D11), AAC 8-1–AAC 8-15, 2002.

Rozanov, V. V., Buchwitz, M., Eichmann, K. U., de Beek, R., Burrows, J. P.: SCIATRAN – a new radiative transfer model for geophysical applications in the 240–2400 nm spectral region: the pseudo-spherical version, Adv. Space. Res., 29 (11), 1831–1835, https://doi.org/10.1016/S0273-1177(02)00095-9, 2002.

Rozanov, V. V.: Adjoint radiative transfer equation and inverse problems, in: Kokhanovsky, A. A. (Eds.), Light Scattering Reviews: Single and Multiple Light Scattering. Springer Berlin Heidelberg, Berlin, Heidelberg, pp. 339-392, https://doi.org/10.1007/3-540-37672-0_8, 2006.

Rozanov, V.V. and Rozanov, A.V.: Relationship between different approaches to derive weighting functions related to atmospheric remote sensing problems, J. Quant. Spectrosc. Ra., 105(2), 217-242, https://doi.org/10.1016/j.jqsrt.2006.12.006, 2007.

Rozanov, V. V., Rozanov, A. V., Kokhanovsky, A. A.: Derivatives of the radiation feld and their application to the solution of inverse problems, in: Kokhanovsky, A. A. (Eds.), Light Scattering Reviews 2: Remote Sensing and Inverse Problems. Springer Berlin Heidelberg, Berlin, Heidelberg, pp. 205-265, https://doi.org/10.1007/978-3-540-68435-0_6, 2007.

Rozanov, V.V., Rozanov, A.V., Kokhanovsky, A.A., Burrows, J. P.: Radiative transfer through terrestrial atmosphere and ocean: Software package SCIATRAN, J. Quant. Spectrosc. Ra., 133. 13-71, https://doi.org/10.1016/j.jqsrt.2013.07.004, 2014.

Serreze, M. C., and Barry, R. C.: Processes and impacts of Arctic amplification: A research synthesis, Global Planet. Change, 77, 85–96, doi:10.1016/j.gloplacha.2011.03.004, 2011.

Schaepman-Strub, G., Schaepman, M. E., Painter, T. H., Dangel, S., Martonchik, J. V.: Reflectance quantities in optical remote sensing-definitions and case studies, Remote Sens. Environ., 103, 27–42, https://doi.org/10.101/j.rs6e.2006.03.002, 2006.

Schneider, S.H. and Dickinson, R. E., Climate modeling, Rev. Geophys., 12, 447-493, https://doi.org/10.1029/RG012i003p00447, 1974.

Shultz, M. J.: Crystal growth in ice and snow, Phys. Today., 71, 35–39, https://doi.org/10.1063/PT.3.3844, 2018.

Sinnhuber, B. M., Sheode, N., Sinnhuber, M., Chipperfield, M. P., Feng, W.: The contribution of anthropogenic bromine emissions to past stratospheric ozone trends: a modelling study, Atmos. Chem. Phys., 9, 2863–71, https://doi.org/10.5194/acp-9-2863-2009, 2009.

Slater, B., and Michaelides, A.: Surface premelting of water ice. Nature Reviews Chemistry, 3:3, 172-188, https://doi.org/10.1038/s41570-019-0080-8, 2019.

Soulen, P. F., King, M. D., Tsay, S. C., Arnold, G. T., Li, J. Y.: Airborne spectral measurements of surface-atmosphere anisotropy during the SCAR-A, Kuwait oil fire, and TARFOX experiments, J. Geophys. Res., 105, 10203–10218, https://doi.org/10.1029/1999JD901115, 2000.

Udisti, R., Traversi, R., Becagli, S., Tomasi, C., Mazzola, M., Lupi, A., and Quinn, P. K. : Arctic Aerosols in: Physics and Chemistry of the Arctic Atmosphere, edited by: Kokhanovsky, A. A., Tomasi, C., Springer Nature Switzerland AG, Cham, Switzerland, 2020.

Warren, S. G.: Optical Properties of Snow, Rev. Geophys. Space Ge., 20, 67–89, https://doi.org/10.1029/RG020i001p00067, 1982.

Warren, S. G., Brandt, R. E., Hinton P. O. R.: Effect of surface roughness on bidirectional reflectance of Antarctic snow, J. Geophys. Res., 103:25789–807, https://doi.org/10.1029/98JE01898, 1998.

Weber, M., Coldewey-Egbers, M., Fioletov, V. E., Frith, S. M., Wild, J. D., Burrows, J. P., Long, C. S., Loyola, D.: Total ozone trends from 1979 to 2016 derived from five merged observational datasets – the emergence into ozone recovery, Atmos. Chem. Phys., 18, 2097-2117, https://doi.org/10.5194/acp-18-2097-2018, 2018.

Wendisch, M., Brückner, M., Burrows, J. P., Crewell, S., Dethloff, K., Ebell, K., Lüpkes, C., Macke, A., Notholt, J., Quaas, J., Rinke, A., and Tegen, I.: Understanding causes and effects of rapid warming in the Arctic, Eos, 98, 22–26, https://doi.org/10.1029/2017EO064803, 2017.

Wendisch, M., Macke, A., Ehrlich, A., Lüpkes, C., Mech, M., Chechin, D., Dethloff, K., Barrientos, C., Bozem, H., Brückner, M., Clemen, H. C., Crewell, S., Donth, T., Dupuy, R., Dusny, C, Ebell, K., Egerer, U., Engelmann, R., Engler, C., Eppers, O., Gehrmann, M., Gong, X., Gottschalk, M., Gourbeyre, C., Griesche, H., Hartmann, J., Hartmann, M., Heinold, B., Herber, A., Herrmann, H., Heygster, G., Hoor, P., Jafariserajehlou, S., Jäkel, E., Järvinen, E., Jourdan, O., Kästner, U., Kecorius, S., Knudsen, E.M., Köllner, F., Kretzschmar, J., Lelli, L., Leroy, D., Maturilli, M., Mei, L., Mertes, S., Mioche, G., Neuber, R., Nicolaus, M., Nomokonova, T., Notholt, J., Palm, M., van Pinxteren, M., Quaas, J., Richter, P., Ruiz-Donoso, E., Schäfer, M., Schmieder, K., Schnaiter, M., Schneider, J., Schwarzenböck, A., Seifert, P., Shupe, M.D., Siebert, H., Spreen, G., Stapf, J., Stratmann, F., Vogl, T., Welti, A., Wex, H., Wiedensohler, A., Zanatta, M., Zeppenfeld, S.: The Arctic Cloud Puzzle: Using ACLOUD/PASCAL Multi-Platform Observations to Unravel the Role of Clouds and Aerosol Particles in Arctic Amplification, Bull. Amer. Meteor. Soc., 100 (5), 841–871, doi:10.1175/BAMS-D-18-0072.1, 2019.

Wiscombe, W. J. and Warren, S. G.: A model for the spectral albedo of snow. I. Pure snow, J. Atmos. Sci., 37, 2712–2733, https://doi.org/10.1175/1520-0469(1980)037<2712:AMFTSA>2.0.CO;2, 1980.

Yang, P. and Liou, K. N.: Single-scattering properties of complex ice crystals in terrestrial atmosphere, Contr. Atmos. Phys., 71, 223–248, 1998.

Yang, P., Baum, B. A., Heymsfield, A. J., Hu, Y. X., Huang, H. L., Tsay, S. C., Ackerman, S.: Single-scattering properties of droxtals, J. Quant. Spectrosc. Ra., 79–80, 1159–1169, https://doi.org/10.1016/S0022-4073(02)00347-3, 2003.

Yang, P., Bi, L., Baum, B. A., Liou, K., Kattawar, G. W., Mishchenko, M. I., Cole, B.: Spectrally Consistent Scattering, Absorption, and Polarization Properties of Atmospheric Ice Crystals at Wavelengths from 0.2 to 100 μm, J. Atmos. Sci., 70, 330–347, https://doi.org/10.1175/JAS-D-12-039.1, 2013.

Zhuravleva, T. B., Kokhanovsky, A. A.: Influence of surface roughness on the reflective properties of snow, J. Quant. Spectrosc. Ra., 112(8), 1353-1368, https://doi.org/10.1016/j.jqsrt.2011.01.004, 2011.

Table1. Summary of the CAR, AERONET aerosol optical thickness (transferred from 0.5 to 0.55 μm) and WFDOAS ozone data used in this study.

Dataset number	1	2	3	4
Date	7th April 2008	7th April 2008	7th April 2008	15th April 2008
Location	Elson-Lagoon	Elson-Lagoon	Elson-Lagoon	Elson-Lagoon
Flight altitude	206 m	647 m	1700 m	181 m
SZA (θ_0)	70.23°	69.11°	67.78°	62.11°
AOT ($\tau\ 0.55\,\mu m$)	0.11	0.11	0.11	0.15
Total ozone column	416 DU	416 DU	416 DU	463.4 DU

Table2. Summary of CAR wavelengths and bandwidth

Channel number	Central wavelengths in μm	Bandwidth in nm
1	0.480	21
2	0.687	26
3	0.340	9
4	0.381	6
5	0.870	10
6	1.028	4
7	0.609	9
8	1.275	24
9	1.554	33
10	1.644	46
11	1.713	46
12	2.116	43
13	2.203	43
14	2.324	48

Table 3. Retrieval of physical characteristics of ice crystals with different shape in the case of most roughened habits. Underlined numbers indicate minimum RMSE.

Ice crystal habit	Asymmetry parameter		Retrieved effective radius (μm)		Old snow		Fresh snow	
	Old snow	Fresh snow	Old snow	Fresh snow	Bias (%)	RMSE (%)	Bias (%)	RMSE (%)
Fractal	0.825	0.827	69.37	76.06	3.50	9.75	13.16	14.69
Droxtal	0.856	0.863	94.48	106.95	0.87	25.54	10.10	34.14
Column	0.873	0.877	74.71	80.49	2.17	7.32	12.36	15.72
Hollow column	0.884	0.888	67.32	72.85	2.80	11.15	13.66	15.14
Aggregate of 8 columns	0.844	0.849	98.83	107.62	2.79	6.97	11.85	18.27
Plate	0.923	0.942	38.93	61.44	-0.44	21.47	11.68	16.99
Aggregate of 5 plates	0.874	0.877	78.02	83.41	1.82	10.34	11.23	12.85
Aggregate of 10 plates	0.893	0.893	65.36	69.28	2.34	13.91	11.52	13.16
Hollow-bullet rosette	0.887	0.889	67.01	73.28	2.16	9.99	12.71	15.16

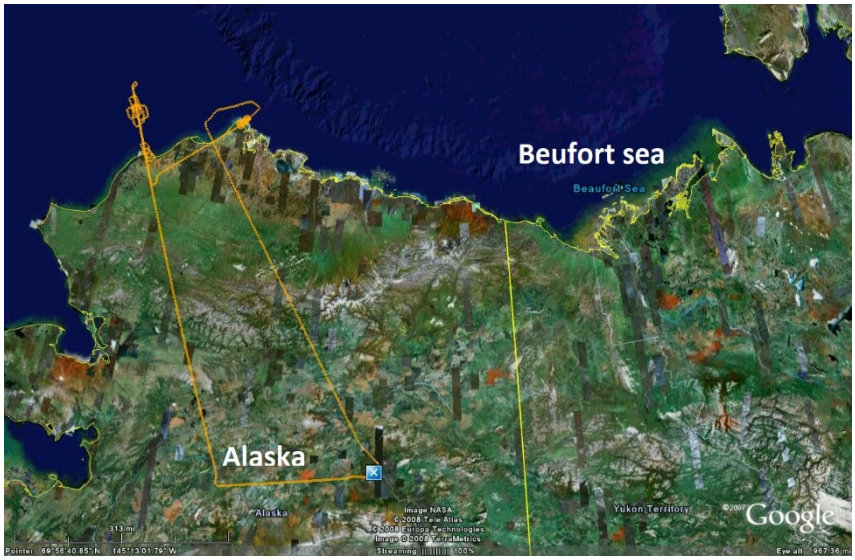

Figure 1: Flight track of P-3B airplane carrying CAR on 07.04.2008 during ARCTAS campaign (Credit: NASA).

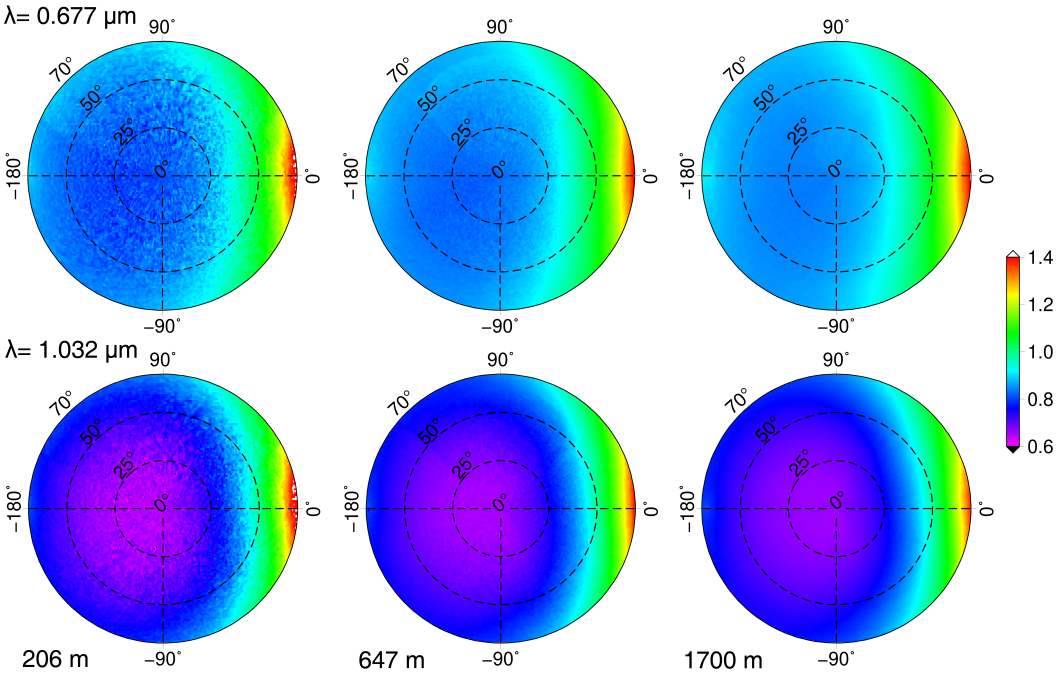

Figure 2: Angular distribution of reflectance factor in the snow-atmosphere system derived from CAR measurements on 7th of April 2008, at Elson Lagoon (71.3° N, 156.4° W): Upper panel at 0.677 μm wavelength and 3 flight altitudes: 206, 647 and 1700 m, respectively; lower panel at 1.032 μm wavelength and at the same flight altitudes. The principal plane is the horizontal line (φ = 0° and 180°), viewing zenith angle is shown as the radius of polar plots from 0° (nadir) to 70°, solar zenith angle is 70.23°, 69.11° and 67.78° for flight altitude of 206, 647 and 1700 m respectively.

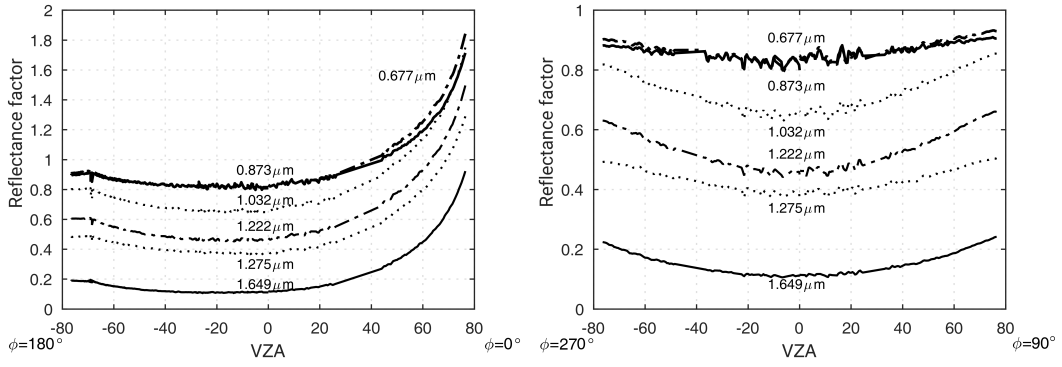

Figure 3: Angular distribution of reflectance factor in the snow-atmosphere system, derived from measurements by CAR at 647 m flight altitude and six wavelengths: 0.677 µm, 0.873 µm, 1.032 µm, 1.222 µm, 1.275 µm and 1.649 µm, on 7th of April 2008, at Elson Lagoon (71.3° N, 156.4° W); left panel: in the principal plane (φ = 0° and 180°) and right: cross plane (φ = 90° and 270°).

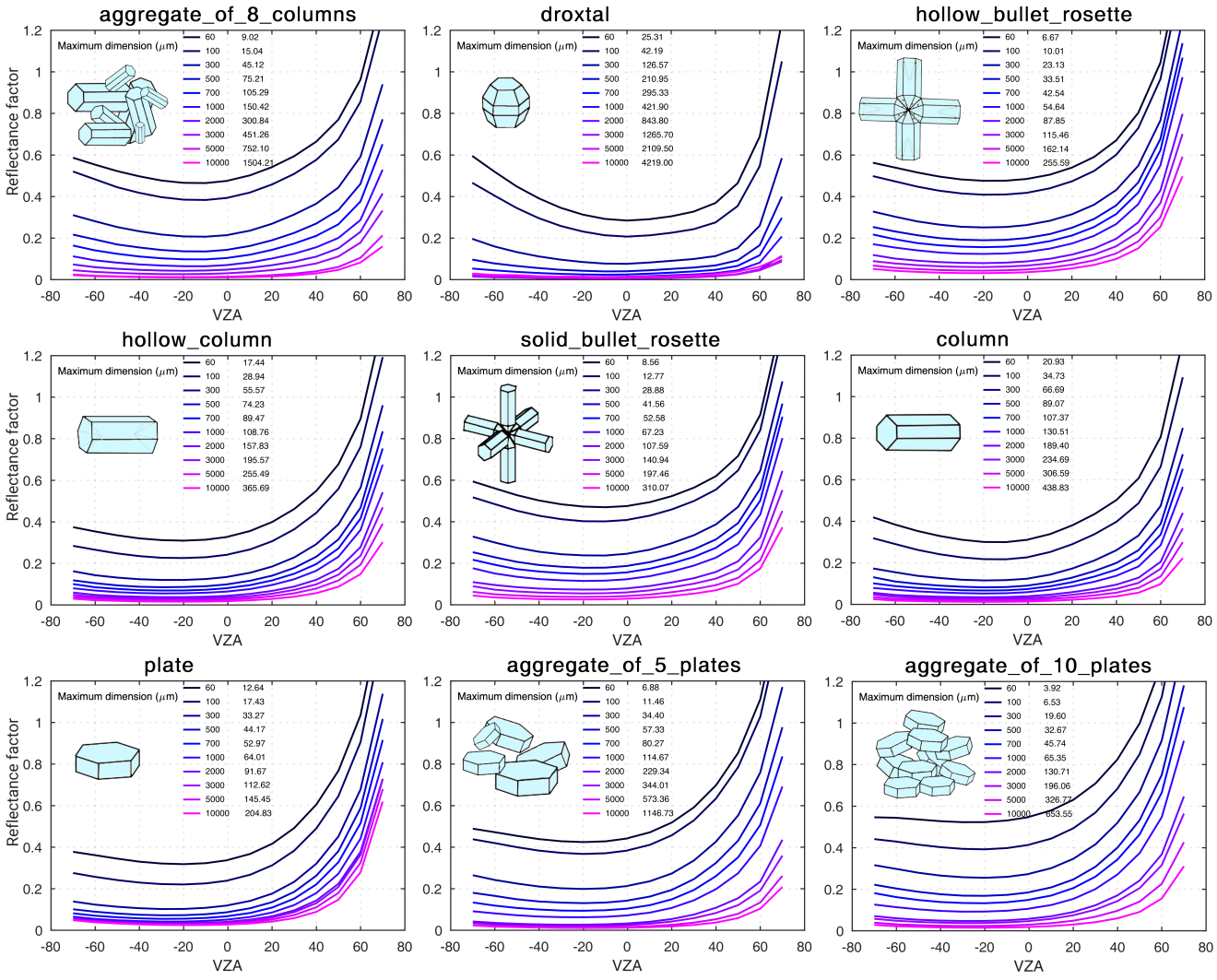

Figure 4: The change of reflectance factor values in principal plane (φ = 0° and 180°) with size and shape of ice crystals at the wavelength of 1.649 μm-, left column in each figure shows the maximum length of ice crystal and right column is its equivalent effective radius.

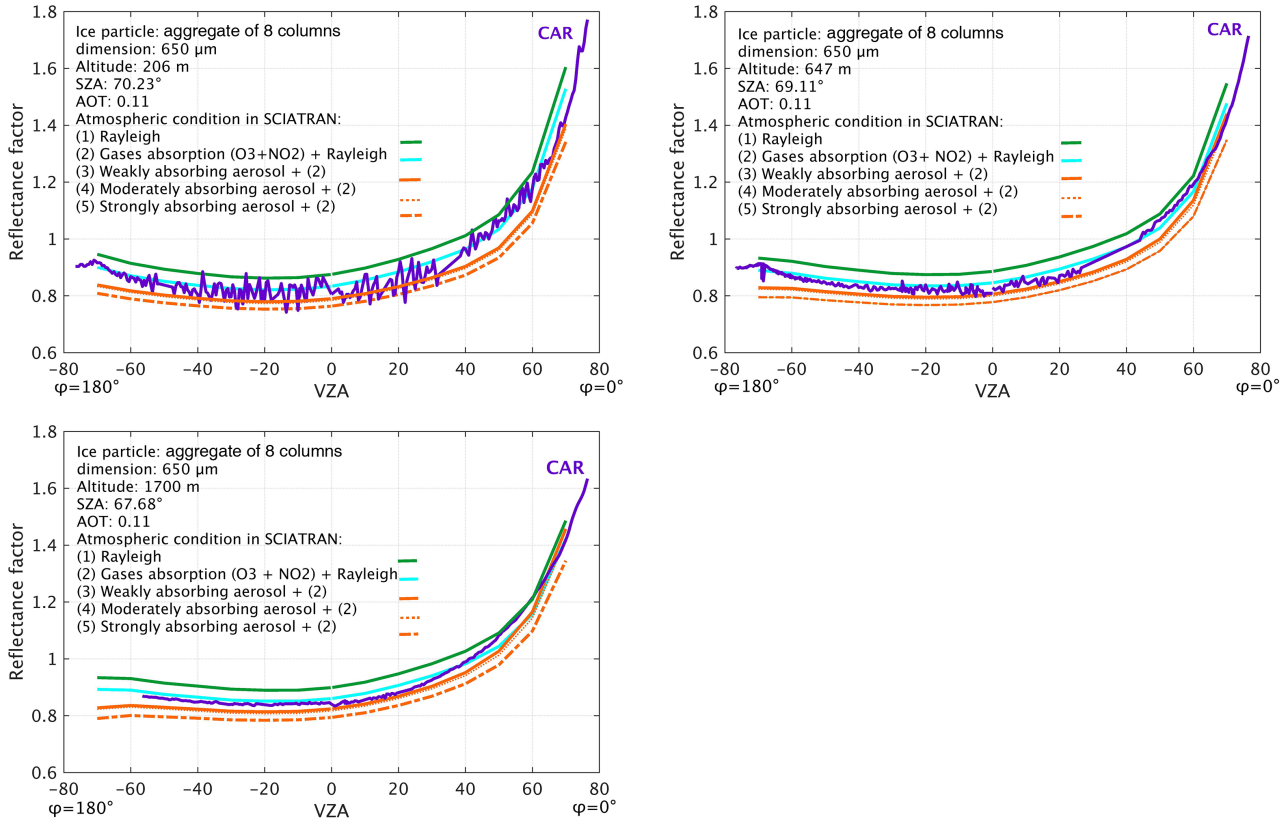

Figure 5: Measured and simulated reflectance factor at 0.677 µm versus VZA in the principal plane (φ = 0° and 180°) at three different flight altitudes. Upper left, upper right and the lower left panel represent results at 206, 647 and 1700 m flight altitude respectively. The green lines indicate simulated reflectance assuming Rayleigh scattering (case i); the blue line shows reflectance for case ii (as case i including absorption of O_3 and NO_2, the orange lines show the reflectance for case iii (as case ii but adding aerosol with an AOT of 0.11 for three types of aerosol: i) weakly absorbing, ii) moderately absorbing and iii) strongly absorbing).

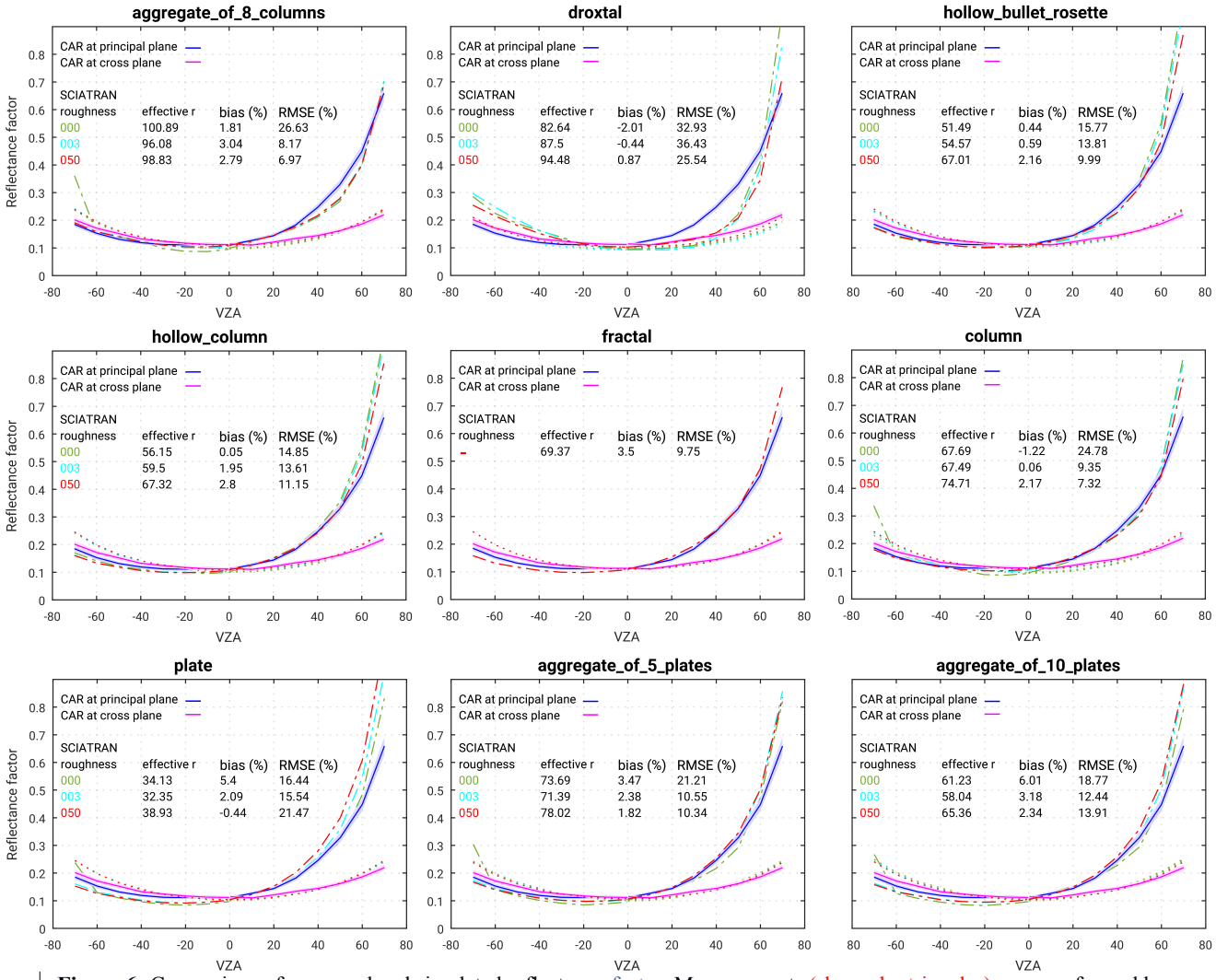

Figure 6: Comparison of measured and simulated reflectance factor. Measurements ~~(shown by triangles)~~ were performed by the CAR instrument over old snow at 647 m flight altitude on the 7th of April 2008 at 1.649 µm. The uncertainty in CAR measurements is indicated by envelope. SCIATRAN simulations in the principal and cross plane given by the dashed-dotted and dotted lines respectively by different colors: green, blue and red present smooth, moderately roughened and severely roughened crystal surface. Positive and negative VZAs correspond to azimuthal angles $\varphi = 0°$ and 180° for principal plane and $\varphi = 90°$ and 270° for perpendicular plane respectively.

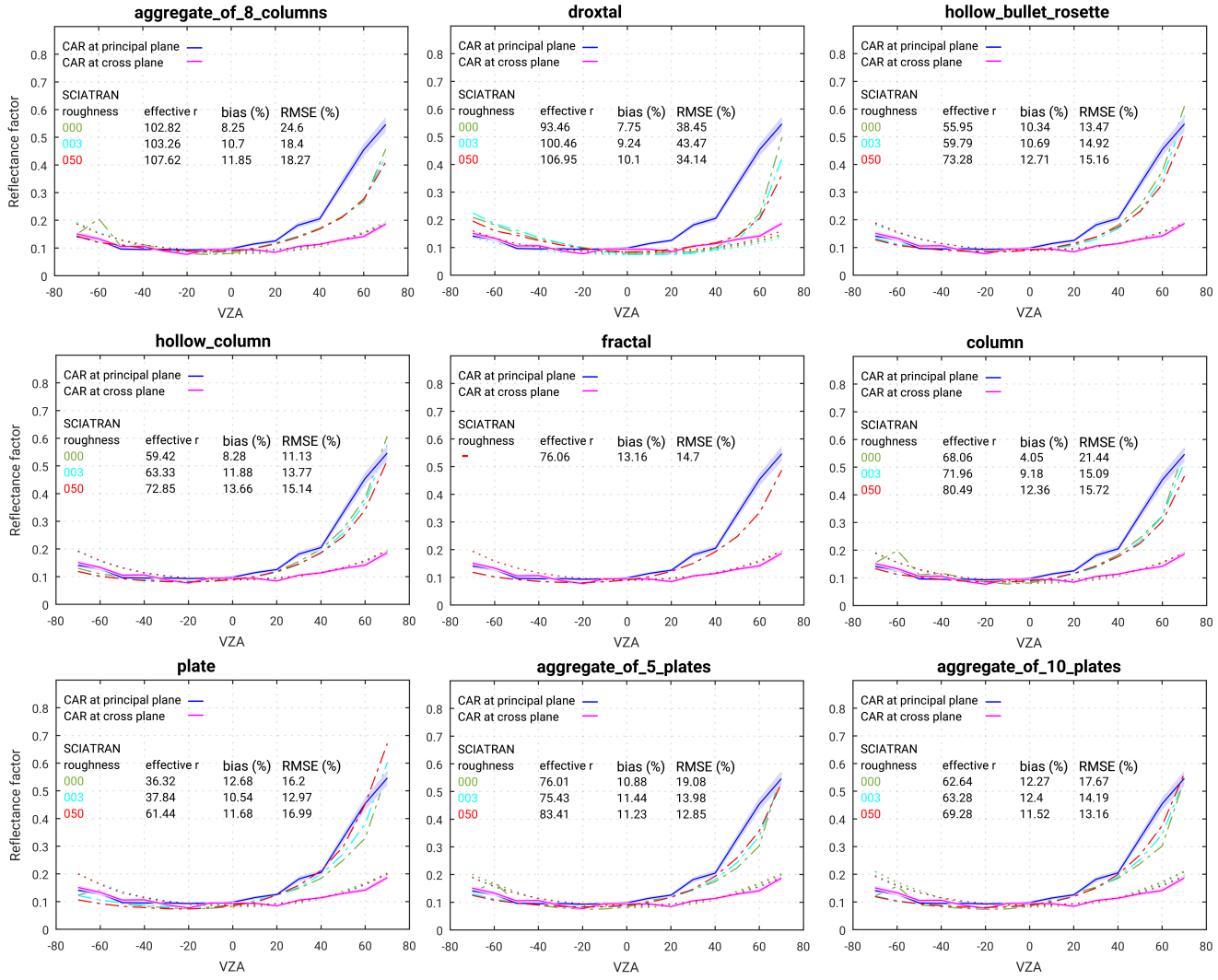

Figure 7: The same as Fig. ~~5~~6 but the measurements by the CAR instrument were performed on the 15th April at 181 m flight altitude over fresh snow.

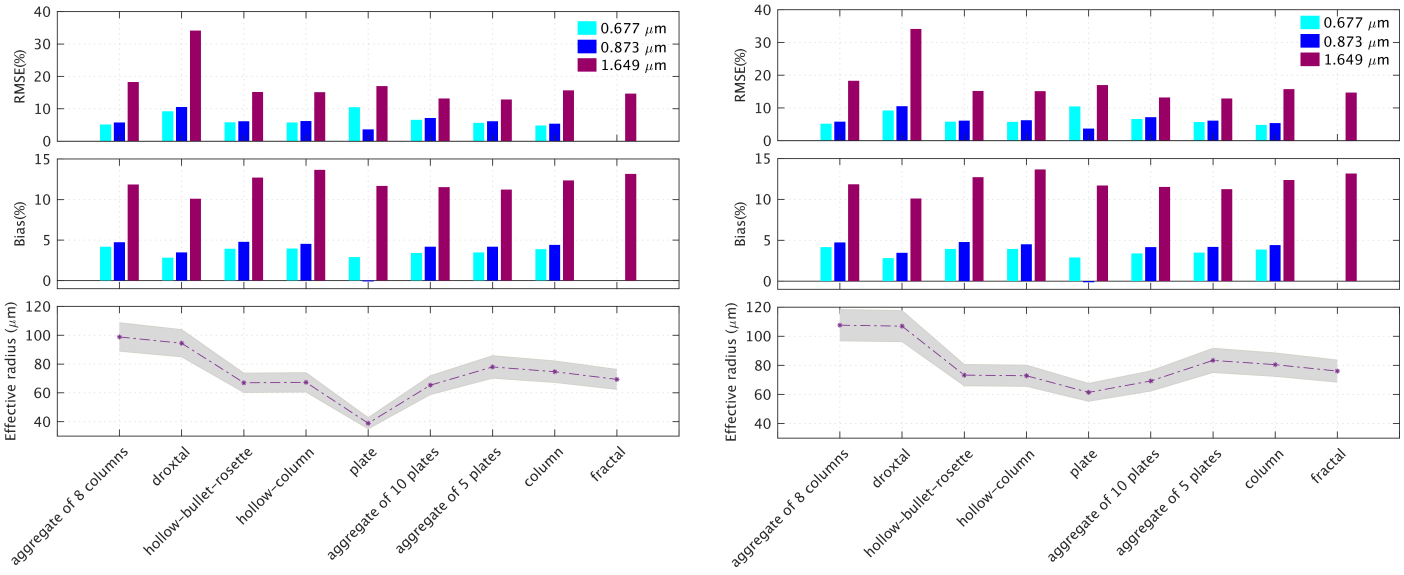

Figure 8: Comparison of snow grain size retrieval and best fit of reflectance at three wavelengths: 0.677, 0.873 and 1.649 µm, left panel: old snow case and right panel: fresh snow case. Effective radius is retrieved at 1.649 µm and grey envelope shows the uncertainty in the retrieved effective radius.

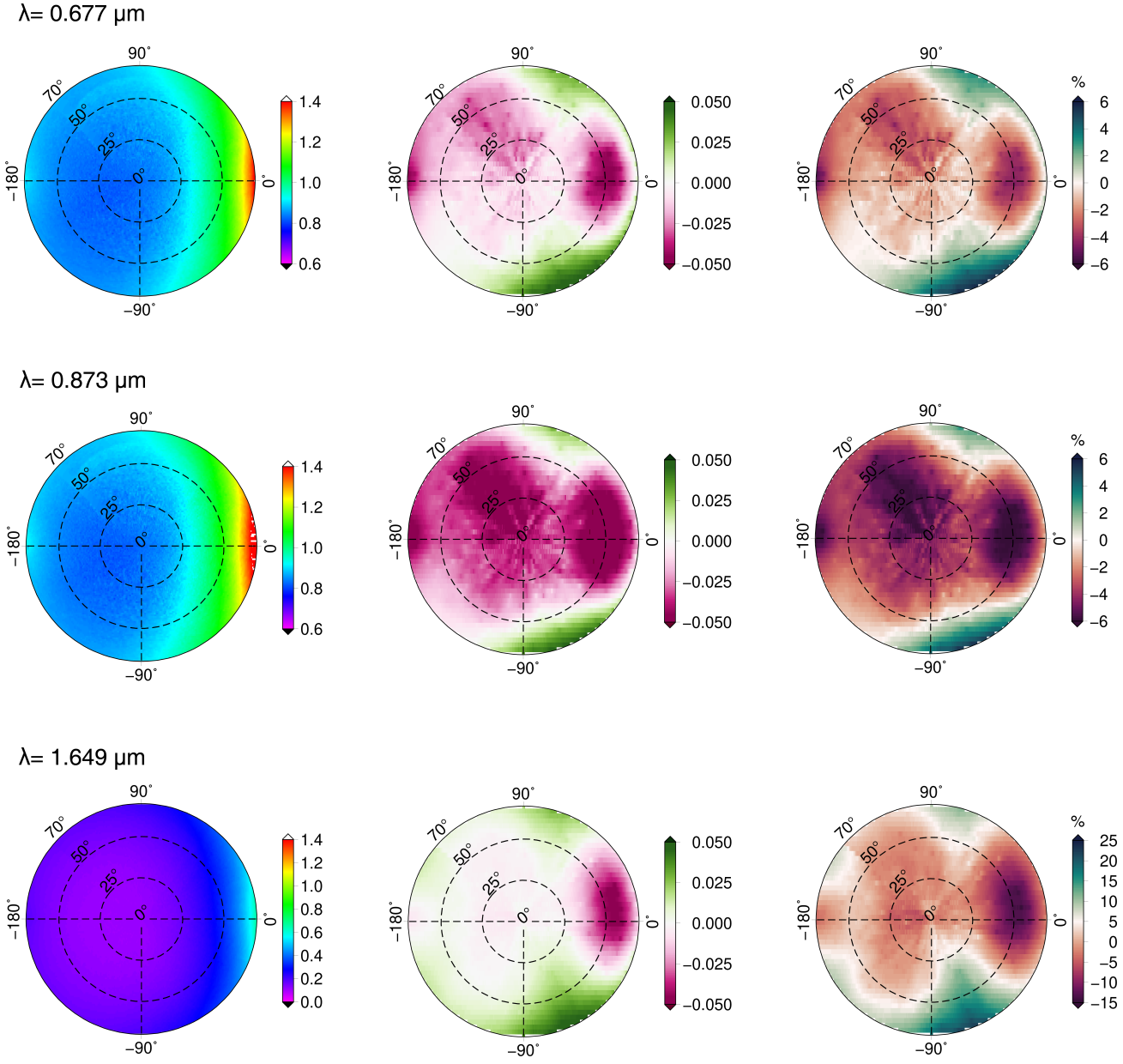

Figure 9: Left column shows reflectance factor at three wavelengths: 0.677, 0.873 and 1.649 μm from the CAR measurements acquired on 7th of April 2008, at Barrow/Utqiaġvik Alaska at an altitude of 647 m; The middle column depicts the absolute difference between simulation and measurement: (RSCIATRAN – RCAR); The right column shows the relative difference in (%).

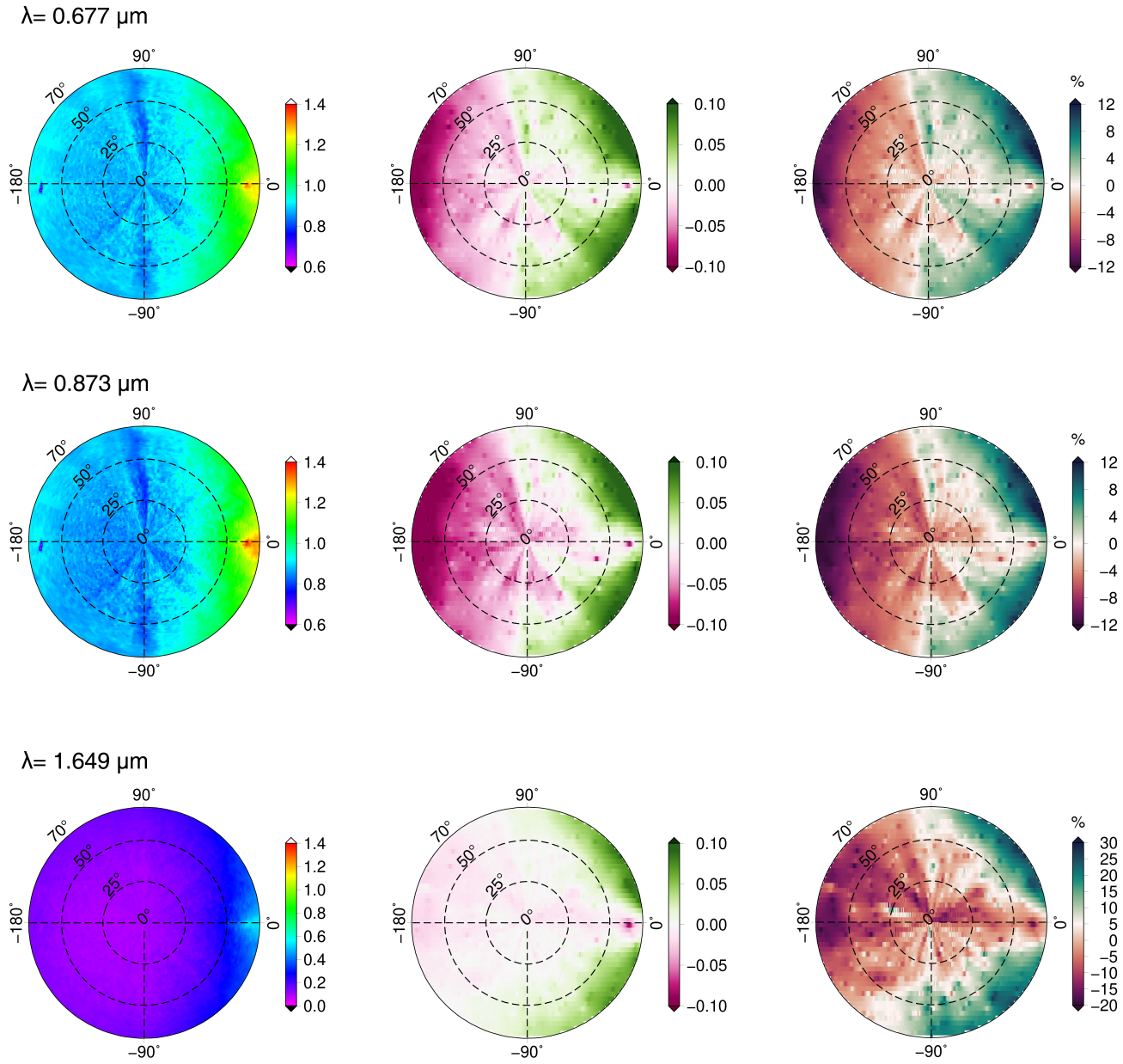

Figure 10: The same as Fig. 98 but the measurements by CAR instrument were performed on 15th April 2008 at 181 m flight altitude over fresh snow.

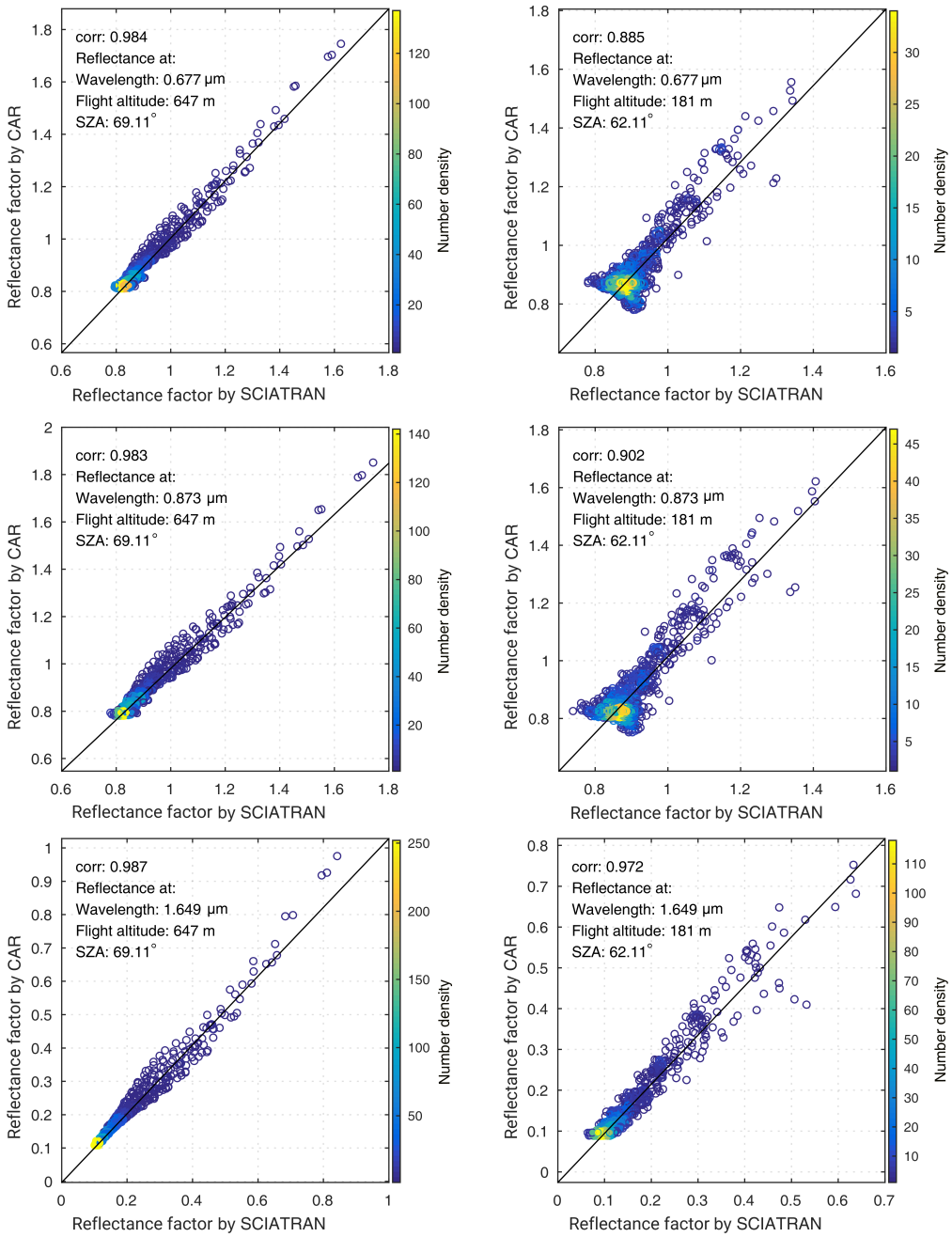

Figure 11: The scatter plot with corresponding Pearson correlation coefficient of reflectance factor measured by CAR and simulated by SCIATRAN; left column shows the results for old snow, right column: fresh snow. ~~h~~Here the color bar represents number density of pixels.